1

Quantum Phase-Space Transport and Applications to the Solid State Physics

Omar Morandi
Institute of Theoretical and Computational Physics, Graz University of Technology
Austria

1. Introduction

Quantum modeling is becoming a crucial aspect in nanoelectronics research in perspective of analog and digital applications. Devices like resonant tunneling diodes or graphene sheets are examples of solid state structures that are receiving great importance in the modern nanotechnology for high-speed and miniaturized systems. Differing from the usual transport where the electronic current flows in a single band, the remarkable feature of this new solid state structures is the possibility to achieve a sharp coupling among states belonging to different bands. Under some conditions, a non negligible contribution to the particle transport induced by interband tunneling can be observed and, consequently, the single band transport or the classical phase-space description of the charge motion based on the Boltzmann equation are no longer accurate. Different approaches have been proposed for the full quantum description of the electron transport with the inclusion of the interband processes. Among them, the phase-space formulation of quantum mechanics offers a framework in which the quantum phenomena can be described with a classical language and the question of the quantum-classical correspondence can be directly investigated. In particular, the visual representation of the quantum mechanical motion by quantum-corrected phase-plane trajectories is a valuable instrument for the investigation of the particle-particle quantum coherence. However, due to the non-commutativity of quantum mechanical operators, there is no unique way to describe a quantum system by a phase-space distribution function. Among all the possible definitions of quantum phase-space distribution functions, the Wigner function, the Glauber-Sudarshan P and Q functions, the Kirkwood and the Husimi distribution have attained a considerable interest (Lee, 1995). The Glauber-Sudarshan distribution function has turned out to be particularly useful in quantum optics and in the field of solid state physics and the Wigner formalism represents a natural choice for including quantum corrections in the classical phase-space motion (see, for example (Jüngel, 2009)).
This Chapter is intended to present different approaches for modeling the quantum transport in nano-structures based on the Wigner, or more generally, on the quantum phase-space formalism. Our discussion will be focused on the application of the Weyl quantization procedure to various problems. In particular, we show the existence of a quite general multiband formalism and we discuss its application to some relevant cases. In accordance with the Schrödinger representation, where a physical system can be characterized by a set of projectors, we extend the original Wigner approach by considering a wider class of representations. The applications of this formalism span among different subjects: the

multi-band transport and its applications to nano-devices, quasi classical approximations of the motion and the characterization of a system in terms of Berry phases or, more generally, the representation of a quantum system by means of a Riemann manifold with a suitable connection. We discuss some results obtained in this contexts by presenting the major lines of the derivation of the models and their applications. Particular emphasis is devoted to present the methods used for the approximation of the solution. The latter is a particularly important aspect of the theory, but often underestimated: the description of a system in the quantum phase-space usually involves a very complex mathematical formulation and the solution of the equation of motion is only available by numerical approximations. Furthermore, the approximation of the quantum phase-space solution in some cases is not merely a technical trick to depict the solution, but could reveal itself to be a valuable basis for a further methodological investigation of the properties of a system. In the multiband case, some asymptotic procedures devised for the approximation of the quantum Wigner solution have shown a very attractive connection with the Dyson theory of the particle interaction, which allows us to describe the interband quantum transition by means of an effective scattering process (Morandi & Demeio, 2008). Furthermore, the formal connection between the Wigner formalism and the classical Boltzmann approach suggests some direct and general approximations where scattering and relaxation mechanisms can be included in the quantum mechanical framework.

The chapter is organized as follows. In sec. 2 an elementary derivation of the Wigner formalism is introduced. The Wigner function is the basis element of a more general theory denoted by Wigner-Weyl quantization procedure. This is explained in section 3.4 and in sections 3.1. The sections 3.2 and 3.4 are devoted to the application of the Wigner-Weyl formalism to the particle transport in semiconductor structures and in graphene. In section 4 an interesting connection between the diagonalization procedure exposed in section 3.1 and the Berry phase theory is presented. In section 5 a general approximation procedure of the pseudo-differential force operator is proposed. This leads to the definition of an effective force field. Its application in some quantum corrected transport model is discussed. Finally, in section 6, the inclusion of phonon collisions in a quantum corrected kinetic model is addressed and the current evolution in graphene is numerically investigated.

2. Definition of the Wigner function

The quantum mechanical motion of a statistical ensemble of electrons is usually characterized by a trace class function denoted as density matrix. For some practical and theoretical reasons, as an alternative to the use of the density matrix, the system is often described by the so-called quasi-density Wigner function, or equivalently, by using the quantum phase-space formalism. The Wigner formalism, for example, has found application in different areas of theoretical and applied physics. For the simulation of out-of-equilibrium systems in solid state physics, the Wigner formalism is generally preferred to the well investigated density matrix framework, because the quantum phase-space approach offers the possibility to describe various relaxation processes in an simple and intuitive form. Although the relaxation processes are ubiquitous in virtually all the real systems involving many particles or interactions with the environment, from the the microscopical point of view, they are sometime extremely difficult to characterize. The description of a system where the quantum mechanical coherence of the particle wave function is only partially lost or the understanding of how a pure quantum state evolves into a classical object, still constitutes an open challenge for the modern theoretical solid state physics (see for example (Giulini et al., 2003)). On

the contrary, when the particles experience many collisions and their coherence length is smaller than the De Broglie distance, an ensemble of particles can easily be described at the macroscopic level, by using for example diffusion equations (the mathematical literature refers to the "diffusive limit" of a particle gas). A strongly-interacting gas becomes essentially an ensemble of "classical particles" for which position and momentum are well defined function (and no longer operators) of time. The phase-space formalism, reveal itself to be a valuable instrument to fill the gap between this two opposite situations. The microscopic evolution of the system can be described exactly and the close analogy with the classical mechanics can be exploited in order to formulate some reasonable approximations to cope with the relaxation effects. Scattering phenomena can be included at different levels of approximation. The simplest approach is constituted by the Wigner-BGK model, where a relaxation-time term is added to the equation of motion. A more sophisticated model is obtained by the Wigner-Fokker-Plank theory, where the collision are included via diffusive terms. Finally, we mention the Wigner-Boltzmann equation where the particle-particle collisions are modeled by the Boltzmann scattering operator (see i. e. Jüngel (2009) for a general introduction to this methods). Furthermore, systems constituted by a gas where the particles are continuously exchanged with the environment ("open systems") are easily described by the quantum phase-space formalism. It results in special boundary conditions for the quasi-distribution function. In this paragraph, we give an elementary introduction to the Wigner quasi-distribution function and we illustrate some of the properties of the quantum phase-space formalism. A more general discussion will be given in sec. 3. For the sake of simplicity, we consider a spinless particle gas, described by the density matrix $\rho(\mathbf{x}_1, \mathbf{x}_2)$, in the presence of a static potential $V(\mathbf{r})$. Following (Wigner, 1932), we define the quasi-distribution function

$$f(\mathbf{r}, \mathbf{p}, t) = \frac{1}{(2\pi)^d} \int_{\mathbb{R}^d_\eta} \rho\left(\mathbf{r} + \hbar\frac{\boldsymbol{\eta}}{2}, \mathbf{r} - \hbar\frac{\boldsymbol{\eta}}{2}, t\right) e^{-i\mathbf{p}\cdot\boldsymbol{\eta}} \, \mathrm{d}\boldsymbol{\eta} \, . \tag{1}$$

Here, d denotes the dimension of the space. The Wigner description of the quantum motion provides a framework that preserves many properties of the classical description of the particle motion. The equation of motion for the Wigner function writes (explicit calculation can be found for example in (Markowich, 1990))

$$\frac{\partial f}{\partial t} = -\frac{\mathbf{p}}{m} \cdot \nabla_{\mathbf{r}} f + \theta[f] \, , \tag{2}$$

where m is the particle mass and the pseudo-differential operator $\theta[f]$ is

$$\theta[f] = \frac{1}{(2\pi)^d} \int_{\mathbb{R}^d_\eta} \int_{\mathbb{R}^d_{p'}} \mathcal{D}\left(\mathbf{r}, \boldsymbol{\eta}\right) e^{i(\mathbf{p}-\mathbf{p}')\cdot\boldsymbol{\eta}} f(\mathbf{r}, \mathbf{p}') \, \mathrm{d}\boldsymbol{\eta} \, \mathrm{d}\mathbf{p}' \tag{3}$$

$$= \frac{1}{(2\pi)^d} \int_{\mathbb{R}^d_\eta} \mathcal{D}\left(\mathbf{r}, \boldsymbol{\eta}\right) \widetilde{f}(\mathbf{r}, \boldsymbol{\eta}) e^{i\mathbf{p}\cdot\boldsymbol{\eta}} \, \mathrm{d}\boldsymbol{\eta} \, , \tag{4}$$

with

$$\mathcal{D}\left(\mathbf{r}, \boldsymbol{\eta}\right) = \frac{i}{\hbar}\left[U\left(\mathbf{r} + \frac{\hbar}{2}\boldsymbol{\eta}\right) - U\left(\mathbf{r} - \frac{\hbar}{2}\boldsymbol{\eta}\right)\right] \, . \tag{5}$$

Equation (4) shows that the pseudo-differential operator acts just as a multiplication operator in the Fourier transformed space $\mathbf{r} - \boldsymbol{\eta}$. We used the following definition of Fourier transform

$\widetilde{f} = \mathcal{F}_{p\to\eta}[f]$:

$$\widetilde{f} = \int_{\mathbb{R}^d_p} f(\mathbf{r},\mathbf{p}) e^{-i\mathbf{p}\cdot\boldsymbol{\eta}}\, \mathrm{d}\mathbf{p}$$
$$f = \frac{1}{(2\pi)^d} \int_{\mathbb{R}^d_\eta} \widetilde{f}(\boldsymbol{\eta},\mathbf{p}) e^{i\mathbf{p}\cdot\boldsymbol{\eta}}\, \mathrm{d}\boldsymbol{\eta}\ .$$

The remarkable difference between the quantum phase-space equation of motion and the classical analogous (Liouville equation)

$$\frac{\partial f}{\partial t} = -\frac{\mathbf{p}}{m}\cdot\nabla_{\mathbf{r}} f - \mathbf{E}(\mathbf{r})\cdot\nabla_{\mathbf{p}} f\ , \tag{6}$$

is constituted by the presence of the pseudo-differential operator $\theta[f]$ that substitutes the classical force $\mathbf{E} = -\nabla_{\mathbf{r}} U$. The increasing of the complexity encountered when passing from Eq. (6) to Eq. (2) is justified by the possibility to describe all the phase-interference effects occurring between two different classical paths, and thus characterizing completely the particle motion at the atomic scale. The analogies and the differences between the Wigner transport equation and the classical Liouville equation have been the subject of many study and reports (see for example Markowich (1990)). In particular, we can convince ourselves that in the classical limit $\hbar \to 0$, Eq. (2) becomes Eq. (6), by noting that, formally, we have

$$\begin{aligned}\lim_{\hbar\to 0}\theta[f] &= \frac{1}{(2\pi)^d}\int_{\mathbb{R}^d_\eta}\int_{\mathbb{R}^d_{p'}} i\boldsymbol{\eta}\cdot\nabla_{\mathbf{r}} U(\mathbf{r})\, e^{i(\mathbf{p}-\mathbf{p}')\cdot\boldsymbol{\eta}} f(\mathbf{r},\mathbf{p}')\, \mathrm{d}\boldsymbol{\eta}\, \mathrm{d}\mathbf{p}' \\ &= \frac{1}{(2\pi)^d}\nabla_{\mathbf{r}} U\cdot\frac{\partial}{\partial\mathbf{p}}\int_{\mathbb{R}^d_\eta}\int_{\mathbb{R}^d_{p'}} e^{i(\mathbf{p}-\mathbf{p}')\cdot\boldsymbol{\eta}} f(\mathbf{r},\mathbf{p}')\, \mathrm{d}\boldsymbol{\eta}\, \mathrm{d}\mathbf{p}' = \nabla_{\mathbf{r}} U\cdot\frac{\partial}{\partial\mathbf{p}} f(\mathbf{r},\mathbf{p})\ .\end{aligned}$$

This limit was rigorously proved in (Lions & Paul, 1993) and in (Markowich & Ringhofer, 1989), for sufficiently smooth potentials. From the definition of the Wigner function given by Eq. (1), we see that the $\mathbf{L}^2(\mathbb{R}^d_r \times \mathbb{R}^d_p)$ space constitutes the natural functional space where the theoretical study of the quantum phace-space motion can be addressed (Arnold, 2008).
The key properties through which the connection between the Wigner formulation of the quantum mechanics and the classical kinetic theory becomes evident, are the relationship between the Wigner function and the macroscopic thermodynamical quantities of the particle ensemble. In particular, the first two momenta of the Wigner distribution, taken with respect to the $\mathbf{p}$ variable, are

$$n(\mathbf{r},t) = \int_{\mathbb{R}^d_p} f(\mathbf{r},\mathbf{p},t)\ \mathrm{d}\mathbf{p} \tag{7}$$

and

$$J(\mathbf{r},t) = -\frac{q}{m}\int_{\mathbb{R}^d_p} \mathbf{p} f(\mathbf{r},\mathbf{p},t)\ \mathrm{d}\mathbf{p} \tag{8}$$

where n and J denote the particle and the current density, respectively. More generally, the expectation value of a physical quantity described classically by a function of the phase-space $\mathcal{A}(\mathbf{r},\mathbf{p},t)$ (relevant cases are for example the total Energy $\frac{p^2}{2m} + V(\mathbf{r})$ or the linear momentum $\mathbf{p}$), is given by

$$\langle\mathcal{A}\rangle = \int_{\mathbb{R}^d_p} \mathcal{A}(\mathbf{r},\mathbf{p},t) f(\mathbf{r},\mathbf{p},t)\ \mathrm{d}\mathbf{p}\, \mathrm{d}\mathbf{r}\ . \tag{9}$$

This equation reminds the ensemble average of a Gibbs system and coincides with the analogous classical formula.

3. Wigner-Weyl theory

The definition of the Wigner function given in Eq. (1) was introduced in 1932. It appears as a simple transformation of the density matrix. The spatial variable $\mathbf{r}$ of the Winger quasi-distribution function is the mean of the two points $(\mathbf{x}_1, \mathbf{x}_2)$ where the corresponding density matrix is evaluated (for this reason sometime is pictorially defined by "center of mass") and the momentum variable is the Fourier transform of the difference between the same points. The Wigner transform is a simple rotation in the plane $\mathbf{x}_1 - \mathbf{x}_2$, followed by a Fourier transform. Despite the apparently easy and straightforward form displayed by the Wigner transformation, its deep investigation, performed by Moyal (1949), revealed an unexpected connection with the former pioneering work of Weyl (1927), where the correspondence between quantum-mechanical operators in Hilbert space and ordinary functions was analyzed. Furthermore, when the Wigner framework was considered as an autonomous starting point for representing the quantum world, the presence of an internal logic or algebra, becomes evident. The Lie algebra of the quantum phase-space framework is defined in terms of the so-called Moyal $\star-$product, that becomes the key tool of this formalism. The noncommutative nature of the $\star-$product reflects the analogous property of the quantum Hilbert operators. In this context, following Weyl, by the term "quantization procedure" is intended a general correspondence principle between a function $\mathcal{A}(\mathbf{r}, \mathbf{p})$, defined on the classical phase-space, and some well-defined quantum operator $\widehat{\mathcal{A}}(\mathfrak{r}, \mathfrak{p})$ acting on the physical Hilbert space (here, in order to avoid confusion, we indicate by $\mathfrak{r}$ and $\mathfrak{p}$ the quantum mechanical position and the momentum operators, respectively). In quantum mechanics, observables are defined by Hilbert operators. We are interested in deriving a systematical and physically based extension of the concept of measurable quantities like energy, linear and orbital momentum. Due to the non-commutativity of the quantum operators $\mathfrak{r}$ and $\mathfrak{p}$, different choices are possible. In particular, based on the correspondence $\mathcal{A}(r, p) \rightarrow \widehat{\mathcal{A}}(\mathfrak{r}, \mathfrak{p})$, any other operator that differs from $\widehat{\mathcal{A}}(\mathfrak{r}, \mathfrak{p})$ in the order in which the operators $\mathfrak{r}$ and $\mathfrak{p}$ appear, can in principle been used equally well to define a new quantum operator. More specifically, at the Schrödinger level, the "position" and the "momentum" representations are alternative mathematical descriptions of the system, where the position and momentum operators $(\mathfrak{r}, \mathfrak{p})$ are formally substituted by the operators $(\mathbf{r}, -i\hbar\nabla_{\mathbf{r}})$ and $(i\hbar\nabla_{\mathbf{p}}, \mathbf{p})$, respectively. From a mathematical point of view, a clear distinction is made between position and momentum degrees of freedom of a particle (and which are represented by multiplicative or derivative operators). This is in contrast to the classical motion described in the phase-space, where the position and the momentum of a particle are treated equally, and they can be interpreted just as two different degrees of freedom of the system. As it will be clear in the following, the Weyl quantization procedure maintains this peculiarity and, from the mathematical point of view, position and momentum share the same properties.

The most common quantization procedures are the standard (anti-standard) Kirkwood ordering, the Weyl (symmetrical) ordering, and the normal (anti-normal) ordering. In particular, standard (anti-standard) ordering refers to a quantization procedure where, given a function $\mathcal{A}$ admitting a Taylor expansion, all of the $\mathfrak{p}$ operators appearing in the expansion of $\widehat{\mathcal{A}}(\mathfrak{r}, \mathfrak{p})$ follow (precede) the $\mathfrak{r}$ operators. A different choice is made in the Weyl ordering rule where each polynomial of the $\mathbf{p}$ and $\mathbf{r}$ variables is mapped, term by term, in a completely

ordered expression of $\mathfrak{r}$ and $\mathfrak{p}$. The generic binomial $\mathbf{p}^m\mathbf{r}^n$ becomes (see i. e. (Zachos et al., 2005))

$$\mathbf{p}^m\mathbf{r}^n \to \frac{1}{2^n}\sum_{r=0}^{n}\binom{n}{r}\mathfrak{r}^r\mathfrak{p}^m\mathfrak{r}^{n-r} = \frac{1}{2^m}\sum_{r=0}^{m}\binom{m}{r}\mathfrak{p}^r\mathfrak{r}^n\mathfrak{p}^{m-r}\,. \tag{10}$$

Following Cohen, (Cohen, 1966), one can consider a general class of quantization procedures defined in terms of an auxiliary function $\chi(r,p)$. The invertible map (for avoiding cumbersome expressions, the symbol of the integral indicates the integration over the whole space for all the variables)

$$\begin{aligned}\mathcal{A}(\mathbf{r},\mathbf{p}) &\equiv \mathrm{Tr}\left\{\widehat{\mathcal{A}}(\mathfrak{r},\mathfrak{p})\, e^{i(\mathbf{p}\mathfrak{r}+\mathbf{r}\mathfrak{p})}\chi(\mathbf{r},\mathbf{p})\right\}\\ &= \left(\frac{\hbar}{2\pi}\right)^d \int \left\langle \mathbf{r}'+\frac{\boldsymbol{\eta}\hbar}{2}\,\middle|\,\widehat{\mathcal{A}}\,\middle|\,\mathbf{r}'-\frac{\boldsymbol{\eta}\hbar}{2}\right\rangle \chi(\boldsymbol{\mu},\boldsymbol{\eta})e^{i(\mathbf{r}-\mathbf{r}')\cdot\boldsymbol{\mu}-i\mathbf{p}\cdot\boldsymbol{\eta}}\,\mathrm{d}\boldsymbol{\mu}\,\mathrm{d}\boldsymbol{\eta}\,\mathrm{d}\mathbf{r}'\end{aligned} \tag{11}$$

defines the correspondence $\widehat{\mathcal{A}}(\mathfrak{r},\mathfrak{p}) \to \mathcal{A}(\mathbf{r},\mathbf{p})$. Different choices of the function χ describe different rules of association. In particular, if $\widehat{\mathcal{A}}$ is the density operator $\widehat{\rho}$ (representing a state of the system), from Eq. (11) we obtain the quantum distribution function f^χ. One of the main advantages in the application of the definition (11) is that the expectation value of the operator $\widehat{\mathcal{A}}(\mathfrak{r},\mathfrak{p})$ can be obtained by the mean value of the function $\mathcal{A}(\mathbf{r},\mathbf{p})$ under the "measure" f^χ

$$\mathrm{Tr}\left\{\widehat{\mathcal{A}}(\mathfrak{r},\mathfrak{p})\,\widehat{\rho}(\mathfrak{r},\mathfrak{p},t)\right\} = \int \mathcal{A}^\chi(\mathbf{r},\mathbf{p})\, f^\chi(\mathbf{r},\mathbf{p},t)\;\mathrm{d}\mathbf{p}\,\mathrm{d}\mathbf{r}\,.$$

As particular cases, it is possible to recover the definition of the most common quasi-probability distribution functions (classification scheme of Cohen). For example for $\chi = e^{\mp i\frac{\hbar}{2}\mu\eta}$ we obtain the standard $(-)$ or anti-standard $(+)$ ordered Kirkwood distribution function. Hereafter, we limit ourselves to consider the case $\chi = 1$, which gives the Weyl ordering rules. The function f^χ becomes the Wigner quasi-distribution

$$f(\mathbf{r},\mathbf{p}) = \frac{1}{(2\pi)^d}\int \left\langle \mathbf{r}+\frac{\boldsymbol{\eta}\hbar}{2}\,\middle|\,\widehat{\rho}\,\middle|\,\mathbf{r}-\frac{\boldsymbol{\eta}\hbar}{2}\right\rangle e^{-ip\cdot\boldsymbol{\eta}}\,\mathrm{d}\boldsymbol{\eta}\,. \tag{12}$$

The Weyl-Moyal theory provides the mathematical ground and a rigorous link between a phase-space function and a symmetrically ordered operator. More into detail, the correspondence between $\widehat{\mathcal{A}}$ and the function $\mathcal{A}(\mathbf{r},\mathbf{p})$ (called the symbol of the operator) is provided by the map $\mathcal{W}[\mathcal{A}] = \widehat{\mathcal{A}}$ (Folland, 1989)

$$\left(\widehat{\mathcal{A}}h\right)(\mathbf{x}) = \mathcal{W}[\mathcal{A}]\,h = \frac{1}{(2\pi\hbar)^d}\int \mathcal{A}\left(\frac{\mathbf{x}+\mathbf{y}}{2},\mathbf{p}\right) h(\mathbf{y})\, e^{\frac{i}{\hbar}(\mathbf{x}-\mathbf{y})\cdot\mathbf{p}}\,\mathrm{d}\mathbf{y}\,\mathrm{d}\mathbf{p}\,. \tag{13}$$

Here, h is a generic function. The inverse of $\mathcal{W}$ is given by the Wigner transform

$$\mathcal{A}(\mathbf{r},\mathbf{p}) = \mathcal{W}^{-1}\left[\widehat{\mathcal{A}}\right](\mathbf{r},\mathbf{p}) = \int \mathcal{K}_{\mathcal{A}}\left(\mathbf{r}+\frac{\boldsymbol{\eta}}{2},\mathbf{r}-\frac{\boldsymbol{\eta}}{2}\right) e^{-\frac{i}{\hbar}\mathbf{p}\cdot\boldsymbol{\eta}}\,\mathrm{d}\boldsymbol{\eta}\,, \tag{14}$$

where $\mathcal{K}_{\mathcal{A}}(\mathbf{x},\mathbf{y})$ is the kernel of the operator $\widehat{\mathcal{A}}$. Let us now fix an orthonormal basis $\psi = \{\psi_i \mid i = 1,2,\ldots\}$. A mixed state is defined by the density operator $\hat{\mathcal{S}}_\psi$

$$\left(\widehat{\mathcal{S}}_\psi\, h\right)(\mathbf{x}) = \int \rho_\psi(\mathbf{x},\mathbf{x}')h(\mathbf{x}')\,\mathrm{d}\mathbf{x}'$$

whose kernel is the density matrix. In the basis $\{\psi_i\}$

$$\rho_\psi(\mathbf{x},\mathbf{x}') = \sum_{i,j} \rho_{ij}\ \psi_i(\mathbf{x})\overline{\psi}_j(\mathbf{x}')\ , \tag{15}$$

where the overbar means conjugation. The von Neumann equation gives the evolution of the density operator $\widehat{\mathcal{S}}_\psi = \widehat{\mathcal{S}}_\psi(t)$ in the presence of the Hamiltonian $\widehat{\mathcal{H}}$:

$$i\hbar\frac{\partial\widehat{\mathcal{S}}_\psi}{\partial t} = \left[\widehat{\mathcal{H}},\widehat{\mathcal{S}}_\psi\right] \tag{16}$$

where, as usual, the brackets denote the commutator. The equivalent quantum phase-space evolution equation can be obtained by applying the Wigner transform. We obtain

$$i\hbar\frac{\partial f_\psi}{\partial t} = \left[\mathcal{H}, f_\psi\right]_\star = \mathcal{H}\star f_\psi - f_\psi\star\mathcal{H} \tag{17}$$

where the symbol $(2\pi\hbar)^d f_\psi(\mathbf{r},\mathbf{p}) \equiv \mathcal{S}_\psi = \mathcal{W}^{-1}\left[\hat{\mathcal{S}}_\psi\right]$ is the Wigner transform of $\rho_\psi(\mathbf{x},\mathbf{x}')$ (see Eq. (1) and Eq. (12)) and we used the following fundamental property

$$\mathcal{W}^{-1}\left[\widehat{\mathcal{A}}\,\widehat{\mathcal{B}}\right] = \mathcal{A}\star\mathcal{B}. \tag{18}$$

For symbols sufficiently regular, the star-Moyal product $\star$ is defined as

$$\begin{aligned}
\mathcal{A}\star\mathcal{B} &\equiv \mathcal{A}\, e^{\frac{i\hbar}{2}\left(\overleftarrow{\nabla}_\mathbf{r}\cdot\overrightarrow{\nabla}_\mathbf{p} - \overleftarrow{\nabla}_\mathbf{p}\cdot\overrightarrow{\nabla}_\mathbf{r}\right)}\ \mathcal{B} \\
&= \sum_n \left(\frac{i\hbar}{2}\right)^n \frac{1}{n!}\mathcal{A}(\mathbf{r},\mathbf{p})\left[\overleftarrow{\nabla}_\mathbf{r}\cdot\overrightarrow{\nabla}_\mathbf{p} - \overleftarrow{\nabla}_\mathbf{p}\cdot\overrightarrow{\nabla}_\mathbf{r}\right]^n \mathcal{B}(\mathbf{r},\mathbf{p}) \\
&= \sum_n \sum_{k=0}^{n} \left(\frac{i\hbar}{2}\right)^n \frac{(-1)^k}{n!}\binom{n}{k}\mathcal{A}(\mathbf{r},\mathbf{p})\left(\overleftarrow{\nabla}_\mathbf{r}\cdot\overrightarrow{\nabla}_\mathbf{p}\right)^{n-k}\left(\overleftarrow{\nabla}_\mathbf{p}\cdot\overrightarrow{\nabla}_\mathbf{r}\right)^k \mathcal{B}(\mathbf{r},\mathbf{p}),
\end{aligned} \tag{19}$$

where the arrows indicate on which operator the gradients act. The Moyal product can be expressed also in integral form (that extends the definition (19) to simply $\mathbf{L}^2$ symbols):

$$\begin{aligned}
\mathcal{A}\star\mathcal{B} &= \frac{1}{(2\pi)^{2d}}\int \mathcal{A}\left(\mathbf{r}-\frac{\hbar}{2}\boldsymbol{\eta},\mathbf{p}+\frac{\hbar}{2}\boldsymbol{\mu}\right)\mathcal{B}\left(\mathbf{r}',\mathbf{p}'\right)e^{i(\mathbf{r}-\mathbf{r}')\cdot\boldsymbol{\mu}+i(\mathbf{p}-\mathbf{p}')\cdot\boldsymbol{\eta}}\ \mathrm{d}\boldsymbol{\mu}\ \mathrm{d}\mathbf{r}'\ \mathrm{d}\boldsymbol{\eta}\ \mathrm{d}\mathbf{p}' \\
&= \frac{1}{(2\pi)^{2d}}\int \mathcal{A}\left(\mathbf{r}',\mathbf{p}'\right)\mathcal{B}\left(\mathbf{r}+\frac{\hbar}{2}\boldsymbol{\eta},\mathbf{p}-\frac{\hbar}{2}\boldsymbol{\mu}\right)e^{i(\mathbf{r}-\mathbf{r}')\cdot\boldsymbol{\mu}+i(\mathbf{p}-\mathbf{p}')\cdot\boldsymbol{\eta}}\ \mathrm{d}\boldsymbol{\mu}\ \mathrm{d}\mathbf{r}'\ \mathrm{d}\boldsymbol{\eta}\ \mathrm{d}\mathbf{p}'\ .
\end{aligned}$$

In particular, if both operators depend only on one variable ($\mathbf{r}$ or $\mathbf{p}$), the Moyal product becomes the ordinary product. For a one-dimensional system the Moyal product simplifies

$$\mathcal{A}\star\mathcal{B} = \sum_{k=0}^{\infty}\frac{\hbar^k}{(2i)^k}\sum_{|\alpha|+|\beta|=k}\frac{(-1)^{|\alpha|}}{\alpha!\beta!}\left(\partial_r^\alpha\partial_p^\beta\mathcal{A}\right)\left(\partial_p^\alpha\partial_r^\beta\mathcal{B}\right) \tag{20}$$

and

$$\begin{aligned}
[\mathcal{A},\mathcal{B}]_\star = \sum_{k=1,3,5,\ldots}^{\infty}\frac{\hbar^k}{(2i)^k}\sum_{0<\beta<k/2}\frac{2(-1)^{\beta+1}}{(k-\beta)!\beta!}\Big[&\left(\partial_r^{k-\beta}\partial_p^\beta\mathcal{A}\right)\left(\partial_p^{k-\beta}\partial_r^\beta\mathcal{B}\right) \\
&-\left(\partial_r^{k-\beta}\partial_p^\beta\mathcal{B}\right)\left(\partial_p^{k-\beta}\partial_r^\beta\mathcal{A}\right)\Big].
\end{aligned}$$

3.1 Generalization of the Wigner-Moyal map

A separable Hilbert space can be characterized by a complete set of basis elements ψ_i or, equivalently, by a unitary transformation Θ (defined in terms of the projection of the ψ_i set on a reference basis). The class of unitary operators $\mathcal{C}(\Theta)$ defines all the alternative sets of basis elements or "representations" of the Hilbert space. Once a representation is defined, the relevant physical variables and the quantum operator can be explicitly addressed. Unitary transformations are a simple and powerful instrument for investigating different and equivalent mathematical formulations of a given physical situation. We study the modification of the explicit form of the Hamiltonian $\mathcal{H}$ (and thus of the equation of motion (17)), induced by a unitary transformation. We consider a unitary operator $\widehat{\Theta}$ and the "rotated" orthonormal basis $\varphi = \{\varphi_i \mid i = 1, 2, \ldots\}$, where $\varphi_i = \widehat{\Theta}\ \psi_i$. It is easy to verify that the following property

$$\Theta^{-1}(\mathbf{r}, \mathbf{p}) = \overline{\Theta}(\mathbf{r}, \mathbf{p}), \tag{21}$$

holds true, where, according to Eq. (14), Θ (Θ^{-1}) is the Weyl symbol of $\widehat{\Theta}$ ($\widehat{\Theta}^{-1}$). The phase-space representation of the state under the unitary transformation $\widehat{\Theta}$ will be denoted by
$(2\pi\hbar)^d f_\varphi \equiv \mathcal{W}^{-1}\left[\widehat{\mathcal{S}}_\varphi\right]$, where

$$\widehat{\mathcal{S}}_\varphi = \widehat{\Theta}\ \widehat{\mathcal{S}}_\psi\ \widehat{\Theta}^\dagger. \tag{22}$$

is the new density operator of the system. Here, the dagger denotes the adjoint operator. By using Eq. (21) it is immediate to verify that the equation of motion for f_φ is still expressed by Eq. (17) with the Hamiltonian $\mathcal{H}' = \Theta \star \mathcal{H} \star \Theta^{-1}$. Explicitly, $\mathcal{H}' \equiv \mathcal{W}^{-1}\left[\widehat{\Theta}\ \widehat{\mathcal{H}}\ \widehat{\Theta}^\dagger\right]$ is given by

$$\mathcal{H}'(\mathbf{r}, \mathbf{p}) = \frac{1}{(2\pi\hbar)^{2d}} \int \Theta\left(\frac{\mathbf{r}+\mathbf{r}'+\mathbf{r}''}{2}, \frac{\mathbf{p}+\mathbf{p}'+\mathbf{p}''}{2}\right) \Theta^{-1}\left(\frac{\mathbf{r}+\mathbf{r}'-\mathbf{r}''}{2}, \frac{\mathbf{p}+\mathbf{p}'-\mathbf{p}''}{2}\right) \times$$
$$\mathcal{H}(\mathbf{r}', \mathbf{p}') e^{\frac{i}{\hbar}[(\mathbf{r}-\mathbf{r}')\cdot\mathbf{p}'' - (\mathbf{p}-\mathbf{p}')\cdot\mathbf{r}'']}\, \mathrm{d}\mathbf{r}'\, \mathrm{d}\mathbf{p}'\, \mathrm{d}\mathbf{r}''\, \mathrm{d}\mathbf{p}''. \tag{23}$$

When passing from the position representation (where the basis elements in the Schrödinger formalism are the Dirac delta distributions and where $\widehat{\Theta}$ is the identity operator), to another possible representation, the Hamiltonian operator modifies according to formula (23). Although the mathematical structure of the equation of motion can be strongly affected by such a basis rotation, the distribution function f_φ is always defined in terms of the classical conjugated variables of position and momentum. The generality of this approach is ensured by the bijective correspondence between a generical unitary transformation (describing all the physical relevant basis transformation) and a framework where the description of the problem is a priori in the phase-space.

3.2 Application to multiband structures: graphene

The previous formalism is particularly convenient for the description of quantum particles with discrete degrees of freedom like spin, pseudo-spin or semiconductor band index. The mathematical structure, emerged in sec. 3.1, can be used in order to define a suitable set of r-p-dependent eigenspaces (with a consequent set of projectors) of the "classical-like" Hamiltonian matrix (that in our case is just the symbol of the Hamiltonian operator). Consequently, a "quasi-diagonalized" matrix representation of the Wigner dynamics can be obtained. This special starting point of the phase-space representation, aids to obtain information on the particle transitions among this countable set of eigenspaces. From a

Physical point of view, these transitions could represent, case by case, spin flip, jumping of a particle from conduction to valence band or particle-antiparticle conversion. The analysis performed in sections 3-3.1 providing Eqs. (16)-(23), maintains its validity when $\widehat{\Theta}$, $\widehat{\mathcal{H}}$ are $n \times n$ matrices of operators (and, consequently the symbols Θ, $\mathcal{H}$ are matrices of functions). This for example, is the standard situation for the Schrödinger-Hilbert space of the form $\mathbf{L}^2\left(\mathbb{R}^d_{\mathbf{x}};\mathbb{C}^n\right)$. The only new prescription is to maintain the order in which the operators and symbols appear in the formulae. To concretize to our exposition, we apply the phase-space formalism to graphene and we present the explicit form of the equation of motion.

Graphene is the two-dimensional honeycomb-lattice allotropic form of carbon. Its discovery stimulated a great interest in the scientific community. In fact, this novel functional material displays some unique electronic properties (see for example (Neto et al., 2009) for a general introduction to graphene). In a quite wide range of energy around the Dirac point, electrons and holes propagate as massless Fermions and the Hamiltonian writes (Beenakker et al., 2008)

$$\widehat{\mathcal{H}} = \widehat{\mathcal{H}}_0 + \sigma_0 U(\mathbf{r}) \,, \tag{24}$$

$$\widehat{\mathcal{H}}_0 = -i\, v_F \hbar\, \boldsymbol{\sigma} \cdot \nabla_{\mathbf{r}} = v_F \hbar \begin{pmatrix} 0 & -i\frac{\partial}{\partial x} - \frac{\partial}{\partial y} \\ -i\frac{\partial}{\partial x} + \frac{\partial}{\partial y} & 0 \end{pmatrix} \,, \tag{25}$$

which describes the motion of an electron-hole pair in a graphene sheet in the presence of an external potential $U(\mathbf{r})$. Here, v_F is the Fermi velocity, $\boldsymbol{\sigma} = (\sigma_x, \sigma_y, \sigma_z)$ indicate the Pauli vector-matrix and σ_0 denotes the identity 2×2 matrix. The upper and lower bands are sometimes denoted by pseudo-spin components of the particle, since the Hamiltonian can be interpreted as an effective momentum-dependent magnetic field $\mathbf{h} \propto \boldsymbol{\sigma} \cdot \nabla_{\mathbf{r}}$.

The application of the theory exposed in sec. 3.1 leads us to consider the density operator $\widehat{\mathcal{S}'} \equiv \widehat{\Theta}\ \widehat{\mathcal{S}}\ \widehat{\Theta}^{\dagger}$ where $\widehat{\Theta}(\mathbf{r}, \nabla_{\mathbf{r}})$ is a unitary 2×2 matrix operator. The approach generally adopted for simplifying the description of a quantum system, is the use of a coordinate framework where the Hamiltonian is diagonal. The graphene Hamiltonian contains off-diagonal terms proportional to the momentum. Since position and momentum are non-commuting quantities, it is not possible to diagonalize $\widehat{\mathcal{H}}$ simultaneously in the position and in the momentum space. Anyway, up to the zero order in $\hbar$, an approximate (r-p)-diagonalization of the Hamiltonian can be obtained. We take advantage of the Weyl correspondence principle and consider the symbol $\Theta(\mathbf{r}, \mathbf{p}) \equiv \mathcal{W}^{-1}\left[\widehat{\Theta}\right]$. Here, $\Theta(\mathbf{r}, \mathbf{p})$ is a unitary matrix parametrized by the $\mathbf{r} - \mathbf{p}$ coordinates. It can be used in order to diagonalize the Hamiltonian symbol $\mathcal{H} = v_F\, \boldsymbol{\sigma} \cdot \mathbf{p} + \sigma_0 U(\mathbf{r})$. With

$$\Theta(\mathbf{p}) = \frac{1}{\sqrt{2}} \begin{pmatrix} 1 & \frac{p_x - i p_y}{\sqrt{p_x^2 + p_y^2}} \\ \frac{p_x + i p_y}{\sqrt{p_x^2 + p_y^2}} & -1 \end{pmatrix} \tag{26}$$

we have

$$\Theta \mathcal{H} \Theta^{\dagger} = \Lambda \tag{27}$$

where $\Lambda(\mathbf{p}) = \sigma_z v_F |\mathbf{p}| + U(\mathbf{r})$ is the relativistic-like spectrum of the graphene sheet. The equation of motion for the new Wigner symbol $\mathcal{S}'$ becomes (see (Morandi & Schürrer, 2011)

for the details of the calculation)

$$i\hbar\frac{\partial\mathcal{S}'}{\partial t} = \left[\mathcal{U}' + \Lambda(\mathbf{p}), \mathcal{S}'\right]_\star . \tag{28}$$

The symbol $\mathcal{U}'(\mathbf{r},\mathbf{p})$ is given by

$$\mathcal{U}'(\mathbf{r},\mathbf{p}) = \Theta \star U(\mathbf{r}) \star \Theta^\dagger \tag{29}$$

and writes explicitly as

$$\mathcal{U}'(\mathbf{r},\mathbf{p}) = \frac{1}{(2\pi)^2}\int \Theta\left(\mathbf{p}+\frac{\hbar}{2}\boldsymbol{\mu}\right)\Theta^\dagger\left(\mathbf{p}-\frac{\hbar}{2}\boldsymbol{\mu}\right)U(\mathbf{r}')e^{i(\mathbf{r}-\mathbf{r}')\cdot\boldsymbol{\mu}}\,\mathrm{d}\boldsymbol{\mu}\,\mathrm{d}\mathbf{r}' .$$

We address explicitly the components of $\mathcal{S}'$, by denoting

$$\mathcal{S}' \equiv (2\pi\hbar)^2\begin{pmatrix} f^+(\mathbf{r},\mathbf{p}) & f^i(\mathbf{r},\mathbf{p}) \\ \overline{f^i}(\mathbf{r},\mathbf{p}) & f^-(\mathbf{r},\mathbf{p})\end{pmatrix} . \tag{30}$$

Equation (28) is written in terms of the Moyal commutator and defines implicitly a non-local evolution operator for the matrix-Wigner function $\mathcal{S}'$. It requires the evaluation of infinite-order derivatives with respect to the variables $\mathbf{r}$ and $\mathbf{p}$. The commutators appearing in Eq. (28) can be written in integral form as

$$\left[\Lambda,\mathcal{S}'\right]_\star = \frac{1}{(2\pi)^2}\int\left[\Lambda\left(\mathbf{p}+\frac{\hbar}{2}\boldsymbol{\mu}\right)\mathcal{S}'(\mathbf{r}',\mathbf{p}) - \mathcal{S}'(\mathbf{r}',\mathbf{p})\,\Lambda\left(\mathbf{p}-\frac{\hbar}{2}\boldsymbol{\mu}\right)\right]e^{i(\mathbf{r}-\mathbf{r}')\cdot\boldsymbol{\mu}}\,\mathrm{d}\boldsymbol{\mu}\,\mathrm{d}\mathbf{r}' \tag{31}$$

$$\left[\mathcal{U}',\mathcal{S}'\right]_\star = \frac{1}{(2\pi)^4}\int\left[\mathcal{U}'\left(\mathbf{r}-\frac{\hbar}{2}\boldsymbol{\eta},\mathbf{p}+\frac{\hbar}{2}\boldsymbol{\mu}\right)\mathcal{S}'(\mathbf{r}',\mathbf{p}') - \mathcal{S}'(\mathbf{r}',\mathbf{p}')\,\mathcal{U}'\left(\mathbf{r}+\frac{\hbar}{2}\boldsymbol{\eta},\mathbf{p}-\frac{\hbar}{2}\boldsymbol{\mu}\right)\right] \times e^{i(\mathbf{r}-\mathbf{r}')\cdot\boldsymbol{\mu}+i(\mathbf{p}-\mathbf{p}')\cdot\boldsymbol{\eta}}\,\mathrm{d}\boldsymbol{\mu}\,\mathrm{d}\mathbf{r}'\,\mathrm{d}\boldsymbol{\eta}\,\mathrm{d}\mathbf{p}' . \tag{32}$$

The commutator of Eq. (31) describes the free motion of the electron-hole pairs in the upper and lower conically shaped energy surfaces. When we discard the external potential U, the evolution of the particles f^+ (f^-) belonging to the upper (lower) part of the spectrum is described by

$$\frac{\partial f^\pm}{\partial t} = \pm\frac{1}{(2\pi)^2}\int\left[E\left(\mathbf{p}+\frac{\hbar}{2}\boldsymbol{\mu}\right) - E\left(\mathbf{p}-\frac{\hbar}{2}\boldsymbol{\mu}\right)\right]f^\pm(\mathbf{r}',\mathbf{p})\,e^{i(\mathbf{r}-\mathbf{r}')\cdot\boldsymbol{\mu}}\,\mathrm{d}\boldsymbol{\mu}\,\mathrm{d}\mathbf{r}' . \tag{33}$$

By expanding up to the leading order in $\hbar$, the previous equation reduces to

$$\frac{\partial f^\pm}{\partial t} \simeq \pm v_F\frac{\mathbf{p}}{|\mathbf{p}|}\cdot\nabla_{\mathbf{r}}f^\pm \tag{34}$$

which is equal to the semi-classical free evolution of the two-particle system in the graphene band structure. We emphasize that the usual semi-classical prescription $v_g = \nabla_{\mathbf{p}}E = v_F\frac{\mathbf{p}}{|\mathbf{p}|}$, where v_g is the group velocity, is automatically fulfilled. As expected from a physical point of view, the coupling between the bands arises from the presence of an external field $U(\mathbf{r})$ which

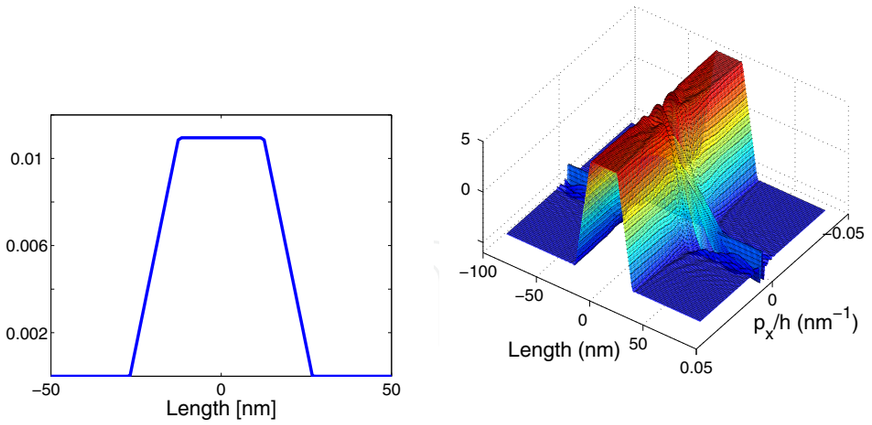

(a) External potential $U(\mathbf{r})$ (b) First component of $\mathcal{U}'(\mathbf{r},\mathbf{p})$

Fig. 1. Comparison between the classical potential U and the momentum dependent pseudo-potential $\mathcal{U}'$.

perturbs the periodic crystal potential. This is described by Eq. (32). In order to illustrate the main characteristics of the pseudo-potential $\mathcal{U}'(\mathbf{r},\mathbf{p})$, in fig. 1 we depict the first component $[\mathcal{U}']_{++}$ of the matrix $\mathcal{U}'$, when the external potential $U(\mathbf{r})$ (represented in the sub-plot 1-(a)) is a single barrier. Equation (29) shows that the elements of the 2×2 matrix $\mathcal{U}'$ depend both on the position $\mathbf{r}$ and the momentum $\mathbf{p}$. The main corrections to the potential arise around $p_x = 0$, whereas $[\mathcal{U}']_{++}$ stays practically identical to U for high values of the momentum p_x. This reflects the presence of the singular behavior of the particle-hole motion in the proximity of the Dirac point (see the discussion concerning this point given in (Morandi & Schürrer, 2011)). The effective potential $[\mathcal{U}']_{++}$ represents the potential "seen" by the particles located in the upper Dirac cone. For small values of p_x, the original squared shape of the potential changes dramatically. The effective potential $[\mathcal{U}']_{++}$ becomes smooth and a long range effective electric field (the gradient of $[\mathcal{U}']_{++}$) is produced. Around $\mathbf{p} = 0$, a barrier or, equivalently, a trap potential becomes highly non-local. It is somehow "spread over the sheet" and, in the case of a trap, its localization effect is greatly reduced.
The equation of motion (28) reproduces the full quantum ballistic motion of the particle-hole gas. In the numerical study presented in (Morandi & Schürrer, 2011b), one of the main quantum transport effects, namely the Klein tunneling, is investigated. The numerical study of the full Wigner system in the presence of a discontinuous potential is presented in (Morandi & Schürrer, 2011). The high computational effort required for solving the full ballistic motion and the need of developing appropriate numerical schemes, limits the practical application of the exact theory. This becomes particularly constraining in view of the simulation of real devices containing dissipative effects like, for example, electron-phonon collisions, that further increase the complexity of the problem. The Wigner formalism is well suited for the inclusion of weak dissipative effects. The overall theoretical and computational complexity displayed by the pseudo-spinorial Wigner dynamics, can be reduced by exploiting some general properties of the system that characterize the application of the multiband Wigner system to real structures (typically, the presence of fast and slow time scaling can be exploited). Approximated models or iterative methods can be derived (see (Morandi & Schürrer, 2011) and (Morandi, 2009) for the application to graphene and to interband diodes, and (Morandi, 2010) for the WKB method in semiconductors).

3.3 Application to multiband structures: correction to the classical trajectory in semiconductors.

We investigate the application of the multiband Wigner formalism to the semiconductor structures. The study of the particle motion in semiconductors has attracted the scientific community, e. g., to the sometime anti-intuitive properties of Bloch waves (especially compared with the classical counterpart). Moreover, the interest has been renewed by the discovery of the unipolar and bipolar junctions and the final impulse to the semiconductor research was given by the unrestrainable progress of the modern industry of electronic devices. An important branch of the semiconductor research is now constituted by the numerical simulation applied to the particle transport. In particular, the continuous miniaturization of field effect transistors (length of a MOS channel approaches the ten nm) imposes the use of a full quantum mechanical (or at least a quantum-correct) model for the correct reproduction of the device characteristic. Beside the Green function formalism and the direct application of the Schrödinger approach, the Wigner framework is a widely employed tool for device simulation. Anyway, most attention is usually devoted to the interband motion since it is often implicitly assumed that electron motion is supported only by one single band. This approximation is based on the assumption that the band-to-band transition probability vanishes exponentially with increasing band gaps (that, for example, in silicon is around one eV), so that under normal conditions all the multiband effects can be discarded. However, this assumption is violated in many heterostructures (devices obtained by connecting semiconductors with different chemical compounds), or when a strong electric field is applied to a normal diode. In both cases electrons are free to flow from one band to another. Beside the evident modification of how the device operates (a new channel for the particle transport becomes available), there is also a more subtle consequence. The application of a strong electric field for example, is able to provide a strong local modification of the electronic spectrum. Since high electric fields could induce a strong mixing of the bands, the Bloch band theory becomes inadequate to describe the particle transport. Even when the particle does not undergo a complete band transition, its motion becomes affected by the interference of the other bands. In the following, we show how these problem can be attacked with the use of the multiband Wigner formalism.

A multiband transport model, based on the Wigner-function approach, was introduced in (Demeio et al., 2006) and in (Unlu et al., 2004) the multiband equation of motion is derived by using the generalized Kadanoff-Baym non-equilibrium Green's function formalism. The model equations there derived are still too hard to be solved numerically. In order to maintain easily the discussion of the problem, we consider a simple model, where only two bands, namely one conduction and one valence band, are retained. We adopt the multiband envelope function model (MEF) described in Ref. (Morandi & Modugno, 2005). This model is derived within the $k \cdot p$ framework and is so far very general. In particular, this approach is focused on the description of the electron transport in devices where tunneling mechanisms between different bands are induced by an external applied bias U. It has been recently applied to some resonant diodes showing self-sustained oscillations (Alvaro & Bonilla, 2010). Under this hypothesis the MEF model furnishes the following Hamiltonian

$$\widehat{\mathcal{H}} = \begin{pmatrix} E_c + U(\mathbf{r}) - \dfrac{\hbar^2}{2m^*}\Delta_{\mathbf{r}} & -\dfrac{\hbar}{m_0}\dfrac{\mathbf{p}_K \cdot \mathcal{E}(\mathbf{r})}{E_g} \\ -\dfrac{\hbar}{m_0}\dfrac{\mathbf{p}_K \cdot \mathcal{E}(\mathbf{r})}{E_g} & E_v + U(\mathbf{r}) + \dfrac{\hbar^2}{2m^*}\Delta_{\mathbf{r}} \end{pmatrix} . \tag{35}$$

Here, E_c (E_v) is the minimum (maximum) of the conduction (valence) energy band, $\mathbf{p}_k$ is the Kane momentum, m_0, m^* are the bare and the effective mass of the electron and U ($\mathcal{E} = \nabla_{\mathbf{r}} U$) is the "external" potential which takes into account different effects, like the bias voltage applied across the device, the contribution from the doping impurities and from the self-consistent field produced by the mobile electronic charge. According to Eq. (27), the multiband system is characterized by the matrix

$$\Theta = \frac{1}{\sqrt{2}} \begin{pmatrix} \sqrt{1+\sigma} & \sqrt{1-\sigma} \\ -\sqrt{1-\sigma} & \sqrt{1+\sigma} \end{pmatrix}, \tag{36}$$

where

$$\sigma = \frac{\Omega}{\sqrt{P_R^2 + \Omega^2}},$$

with $\Omega(\mathbf{p}) = \frac{E_g}{2} + \frac{|\mathbf{p}|^2}{2m^*}$ $P_R(\mathbf{r}) = -\hbar \frac{\mathbf{p}_k \cdot \mathcal{E}(\mathbf{r})}{E_g m_0}$ and $E_g = E_c - E_v$ is the band gap. The eigenvalues of the Hamiltonian are $\mathcal{H}^{\pm}(\mathbf{r}, \mathbf{p}) = \pm\sqrt{P_R^2 + \Omega^2} + U$. Here we limit ourselves to discuss the system obtained by expanding the full quantum equation of motion given in Eq. (28) up to the first order in $\hbar$ (the study of the full quantum system is addressed in (Morandi, 2009)). With the definition (in order to avoid confusion with the graphene Wigner functions defined in Eq. (30), we changed the name of the various components of the matrix)

$$\mathcal{S}' \equiv (2\pi\hbar)^3 \begin{pmatrix} h_c(\mathbf{r}, \mathbf{p}) & h_{cv}(\mathbf{r}, \mathbf{p}) \\ \overline{h_{cv}}(\mathbf{r}, \mathbf{p}) & h_v(\mathbf{r}, \mathbf{p}) \end{pmatrix}. \tag{37}$$

We obtain the following equations of motion

$$\frac{\partial h_c}{\partial t} = -\nabla_{\mathbf{p}} \mathcal{H}^+ \cdot \nabla_{\mathbf{r}} h_c + \nabla_{\mathbf{r}} \mathcal{H}^+ \cdot \nabla_{\mathbf{p}} h_c - 2\xi\, \Re(h_{cv}) \tag{38}$$

$$\frac{\partial h_v}{\partial t} = -\nabla_{\mathbf{p}} \mathcal{H}^- \cdot \nabla_{\mathbf{r}} h_v + \nabla_{\mathbf{r}} \mathcal{H}^- \cdot \nabla_{\mathbf{p}} h_v + 2\xi\, \Re(h_{cv}) \tag{39}$$

$$\frac{\partial h_{cv}}{\partial t} = -\frac{i}{\hbar} \left(\mathcal{H}^+ - \mathcal{H}^-\right) h_{cv} + \mathcal{E} \cdot \nabla_{\mathbf{p}} h_{cv} + \xi \left(h_c - h_v\right) \tag{40}$$

where $\Re$ denotes the real part and

$$\xi = \frac{P_R}{P_R^2 + \Omega^2} \frac{\mathcal{E} \cdot \mathbf{p}}{m^*}. \tag{41}$$

Here, h_c and h_v represent the Wigner quasi-distribution functions of particles in a regime of strong band-to-band coupling. They differ from the analogous functions based on a direct application of the projection of the particle motion in the Bloch basis. The system of Eq. (38)-(40) shows that, up to the zero order in $\hbar$, the Wigner functions h_c (h_v) follows the Hamiltonian flux generated by $\mathcal{H}^+$ $(\mathcal{H}^-)$. Furthermore, the term $\mathcal{H}^+ - \mathcal{H}^- = 2\sqrt{{P_R}^2 + \Omega^2}$ in Eq. (40) induces fast-in-time oscillations (whose frequency is of the order of $E_g/\hbar$) which, up to zero order in $\hbar$, decouple h_{cv} from the slowly varying functions h_c and h_v. This aspect is examined in sec. 3.4. We explore the single band limit of Eqs. (38)-(40). From the physical point of view, we expect that when the electric field goes to zero or the band gap goes to

infinity, all the multiband corrections become negligible and the dynamics of the electrons in the conduction band decouples from those in the valence band. It is convenient to define the parameter $\mathrm{Y} = \frac{P_R}{\Omega}$ that vanishes in the single band limits $\mathcal{E}, 1/E_g \to 0$. When $\mathrm{Y} \to 0$ the evolution of h_c and h_v is described by two Liouville equations (one for each band) with the Hamiltonian

$$\begin{aligned} \mathcal{H}^{\pm} &= \pm\sqrt{{P_R}^2 + \Omega^2} + U(\mathbf{r}) \\ &= \pm\frac{|\mathbf{p}|^2}{2m^*} + U(\mathbf{r}) \pm \frac{E_g}{2}\left(1 + \frac{\Omega}{E_g}\mathrm{Y}^2\right) + o\left(\mathrm{Y}^2\right). \end{aligned} \tag{42}$$

Equation (42) shows that the eigenvalues of the Hamiltonian symbol, provide a simple quantum correction to the classical single band Hamiltonian $\mathcal{H}_{sb} = U(\mathbf{r}) \pm \frac{|\mathbf{p}|^2}{2m^*}$. The particles follow a new trajectory defined by

$$\begin{cases} \dot{\mathbf{r}} = \dfrac{1}{\sqrt{1 + \left(\frac{P_R}{\Omega}\right)^2}}\,\dfrac{\mathbf{p}}{m^*} \\ \dot{\mathbf{p}} = -\mathcal{E} - \dfrac{1}{\sqrt{1 + \left(\frac{\Omega}{P_R}\right)^2}}\,\dfrac{\hbar}{m_0 E_g}\,\nabla_{\mathbf{r}}\left(\mathcal{E}\cdot\mathbf{p}_k\right) \end{cases}. \tag{43}$$

Similar results can be obtained with $\mathcal{H}^-$. Due to the term $\sqrt{1 + \left(\frac{P_R}{\Omega}\right)^2}$, the particles move with a slightly larger effective mass. The mass correction depends on the classical position and momentum. This effect could partially compensate the small effective mass values predicted by the $k \cdot p$ theory in semiconductors with a small band gap like InAs or InSb.

3.4 Study of the band transition, an iterative solution Wigner function

The quasi-diagonal Wigner formalism suggests an interesting analogy between band transition induced by a constant electric field (usually denoted as Zener transition (Zener, 1934)) and the scattering processes. In sec. 3.3 the analysis of the equation of motion was restricted to the single band dynamics. In this section, the full many-band dynamics is treated by means of an iterative procedure. For the sake of simplicity, we consider the two-band system in the presence of a uniform electric field. We introduce the new momentum variable $\mathbf{p}' = \mathbf{p} + \mathcal{E}t$ and we apply the Fourier transformation with respect to the $\mathbf{r}$ variable. The Eqs. (38)-(40) become

$$\frac{\partial g_c}{\partial t} = i\boldsymbol{\mu}\cdot\nabla_{\mathbf{p}}\mathcal{H}^+(t)g_c - \xi(t)\,\left(g_{cv} + g_{vc}\right) \tag{44}$$

$$\frac{\partial g_v}{\partial t} = i\boldsymbol{\mu}\cdot\nabla_{\mathbf{p}}\mathcal{H}^-(t)g_v + \xi(t)\,\left(g_{cv} + g_{vc}\right) \tag{45}$$

$$\frac{\partial g_{cv}}{\partial t} = -\frac{i}{\hbar}2\sqrt{P_R^2 + \Omega^2(t)}\,g_{cv} + \xi(t)\left(g_c - g_v\right) \tag{46}$$

$$\frac{\partial g_{vc}}{\partial t} = \frac{i}{\hbar}2\sqrt{P_R^2 + \Omega^2(t)}\,g_{cv} + \xi(t)\left(g_c - g_v\right), \tag{47}$$

where, in order to avoid confusion, we defined the new unknowns $g_i = \mathfrak{F}_{\mathbf{r}\to\boldsymbol{\mu}}\left[h_i(\mathbf{r}, \mathbf{p} + \mathcal{E}t, t)\right]$ with $i = c, v, cv, vc$. The time dependence of the coefficients is originated by the definition of

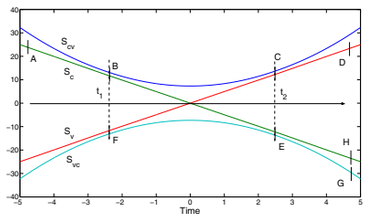

Fig. 2. Eigenvalues of the $\mathfrak{L}$ matrix

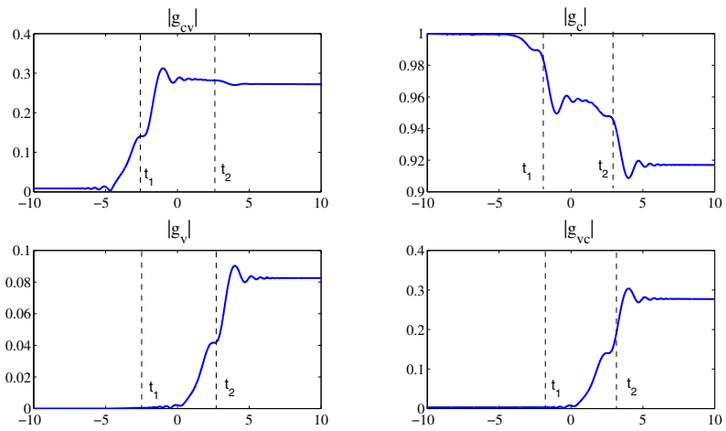

Fig. 3. Modulus of the functions g_i with $i = cv, c, v, vc$.

the $\mathbf{p}'$ variable. Explicitly, $\nabla_{\mathbf{p}}\mathcal{H}^-(t) \equiv \nabla_{\mathbf{p}}\mathcal{H}^-\big|_{\mathbf{p}=\mathbf{p}'-\mathcal{E}t'}$, $\xi(t) \equiv \xi(\mathbf{p} = \mathbf{p}' - \mathcal{E}t)$, and similar for the other coefficients.

The system of Eqs. (44)-(47) is a time-dependent eigenvalue problem with perturbation. In fact, if we define the four component vector $\mathbf{G} = (g_c, g_v, g_{cv}, g_{vc})^t$, Eqs. (44)-(47) can be rewritten as $\frac{\partial \mathbf{G}}{\partial t} = i\mathfrak{L}(t)\mathbf{G} + \mathfrak{T}(t)\mathbf{G}$, where $\mathfrak{L}$ is a diagonal time-dependent matrix and $\mathfrak{T}$ is the perturbation. In order to make the subsequent discussion easier, we define the elements of $\mathfrak{L}$ by $\lambda_c = \boldsymbol{\mu} \cdot \nabla_{\mathbf{p}}\mathcal{H}^+(t)$, $\lambda_v = \boldsymbol{\mu} \cdot \nabla_{\mathbf{p}}\mathcal{H}^-(t)$, $\lambda_{cv} = -\frac{2}{\hbar}\sqrt{P_R^2 + \Omega^2(t)}$ and $\lambda_{vc} = -\lambda_{cv}$ (the coefficients of $\mathfrak{T}$ can be obtained by comparison with Eqs. (44)-(47)). Each function g_i can be identified by the component of $\mathbf{G}$ of the unperturbed eigenvector basis (in this case, the simple canonical basis). The eigenvalues of the matrix $\mathfrak{L}$ are shown in fig. 2.

If we assume that $\mathfrak{L}(t)$ and $\mathfrak{T}$ vary slowly in time, according to well known results of adiabatic perturbation theory, eigenspaces belonging to different eigenvalues are decoupled as long as the difference among the eigenvalues is large. In this case, the projections of the solution on the different eigenspaces evolve independently. Only when the eigenvalues become closer, a coupling is possible and a transition from one eigenspace to another can be performed. In our case, a coupling of the eigenspaces is can be observed only around $t \approx t_1$ and $t \approx t_2$ (see fig. 2).

For the sake of concreteness, we consider a tunneling transition from the conduction band to the valence band. This can be described by setting initially all the functions to zero, with the exception of g_c. As it is customary in the time-dependent perturbation theory, we fix the initial time equal to $-\infty$. The value of g_v for $t \to +\infty$ gives the measure of the interband tunneling

induced by $\mathcal{E}$. We write the solution in terms of the Dyson expansion

$$\mathbf{G}^i = e^{i\int_{-\infty}^{t}\mathfrak{L}(\tau)\,\mathrm{d}\tau}\mathbf{G}_0 + \int_{-\infty}^{t} e^{i\int_{t'}^{t}\mathfrak{L}(\tau)\,\mathrm{d}\tau}\mathfrak{T}(t')\mathbf{G}^{i-1}(t')\,\mathrm{d}t' \tag{48}$$

The integral equation (48) can be easily approximated order by order. The second order writes (we discuss only the valence component of $\mathbf{G}$)

$$g_v^1 = \mathcal{J}_{v,cv} + \mathcal{J}_{v,vc}\,, \tag{49}$$

with

$$\mathcal{J}_{v,vc}(t) = e^{\int_{-\infty}^{t}\lambda_v(\tau)\,\mathrm{d}\tau}\int_{-\infty}^{t}\xi(t')\,e^{\int_{-\infty}^{t'}\lambda_{cv}(\tau)-\lambda_v(\tau)\,\mathrm{d}\tau}g_{cv}^1(t')\;\mathrm{d}t' \tag{50}$$

$$g_{cv}^1(t') = g_c^0\,e^{\int_{-\infty}^{t'}\lambda_c\,\mathrm{d}\tau}\int_{-\infty}^{t'}\xi(t'')\,e^{-\int_{t''}^{t'}(\lambda_c-\lambda_{cv})\,\mathrm{d}\tau}\,\mathrm{d}t''\,. \tag{51}$$

where g_c^0 is the initial condition of g_c. Similar formula holds for $\mathcal{J}_{v,cv}$. We have that $|\lambda_{cv}(t) - \lambda_c(t)| > E_g$, therefore, in a wide gap semiconductor, the only relevant contribution to the integral is generated in the neighborhood of the minimum of the oscillation frequency (for $t \approx t_1$, see fig. 2). Consequently, at $t = t_1$ the g_{cv} function increases sharply (see fig. 3). The integral in Eq. (50) can be approximated in the same manner. Since the minimum of $|\lambda_{cv}(t) - \lambda_v(t)|$ occurs for $t = t_2 > t_1$, g_{cv}^1 can be considered as constant around t_2 and the integral can be estimated by using the stationary phase approximation.

According to these considerations, the time evolution of the system can be described as follows. For $t < t_1$ the solution, which initially belongs to the $\mathcal{S}_c$ eigenspace (we denote with $\mathcal{S}_i$ the eigenspace spanned by the i-th component of $\mathbf{G}$), evolves adiabatically remaining in $\mathcal{S}_c$. As shown in fig. 3, g_c is the only non-vanishing component of the solution $\mathbf{G}$ until $t = t_1$. At $t = t_1$, a very sudden drop of the value of g_c is observed, and, correspondingly, the g_{cv} distribution function increases. This can be interpreted as the creation of an excited state in the g_{cv} band (visualized with the B point in fig. 2). This excited state "moves" in the S_{cv} band until, at $t = t_2$, it generates an S_v state, which is described by the g_v distribution function. The term $\mathcal{J}_{v,cv}$ of Eq. (50) is thus associated with the path $A - B - C - D$ indicated in fig. 2. The particle is initially in the conduction band (represented by the point A) and in B an excited state is created. It moves towards the point C. There it generates a particle in the valence band which moves adiabatically (point D). The inverse of the difference of the eigenvalues ($\lambda_c - \lambda_{cv}$ in t_1 and $\lambda_{cv} - \lambda_v$ in t_2) quantifies the strength of the coupling (or the probability of a transition). The behavior of the function g_c can be described with similar arguments. The g_c function describes the states that move from A (initial time) to H (final time). This distribution undergoes two scattering events, in B (at $t = t_1$) and in E (at $t = t_2$). We note that, at $t = 0$, no scattering phenomena can be observed, since the eigenspaces S_c and S_v are always decoupled. This represents the analogous of the selection rules for the ordinary scattering phenomena.

This iterative procedure resemble very closely the formalism used for the description of the electron scattering phenomena in semiconductors. In our study of interband transitions, this analogy used for the description of the Zener phenomenon in term of a tunneling process where a particle "disappears" from the band where it was initially located, and it "appears" in a different branch of the band diagram. This behaves similarly to the generation of an electron-hole pair induced by the absorption of a photon. This procedure has been exposed more into details in (Morandi & Demeio, 2008). The field dependent case is treated in (Morandi, 2009).

4. Berry phase and Wigner-Weyl formalism

In a crystal where the effective Hamiltonian is expressed by a partially diagonalized basis (e. g. in graphene or in semiconductors), the major particle operators have off-diagonal elements and the usual definitions of the macroscopic quantities, like for example the mean velocity or the particle density, no longer apply. The theory of Berry phases offers an elegant explanation of this effect in terms of the intrinsic curvature of the perturbed band (Bohm et al., 2008; Xiao et al., 2010). We discuss how it is possible to characterize the Berry phase in a multiband system by using our kinetic description of the quantum dynamics.
The Berry phase theory cannot be directly applied to the particle evolution in a graphene sheet for the obvious reason that the Hamiltonian given in Eq. (25) does not contain any adiabatic variable. Anyway, a Berry-like procedure can be developed if we renounce to treat rigorously the particle dynamics and some approximations are retained. From the physical point of view, one of the most interesting properties of the particle-hole pair in graphene is its pseudo-spinorial character and its connection with the orbital motion. In the momentum representation, the unperturbed graphene Hamiltonian writes $v_F\ \boldsymbol{\sigma}\cdot\mathbf{p}$. If we assume that the particle wave function is represented by a non-spreading wave packet centred around the position $\mathbf{r}$ and the momentum $\mathbf{p}$, we expect due to the Ehrenfest theorem that, in the presence of a gentle potential U (sufficiently smooth), the center of mass of such wave function will describe a trajectory $\mathbf{r}(t),\mathbf{p}(t)$. Sometime this is pictorially visualized by saying that the particle is confined in a small box located at a certain position $\mathbf{r}$ and that the wave packet moves without spreading along a certain trajectory $\mathbf{r}(t)$. If we now *assume* that in such situation the graphene Hamiltonian can be approximated by $v_F\ \boldsymbol{\sigma}\cdot\mathbf{p}(t)$, we can treat the momentum trajectory like an external adiabatic variable. It should be noted that since a non-trivial trajectory is always generated by a potential U, this term should be explicitly included in the graphene Hamiltonian as we did in Eq. (24). Anyway, when included, the Hamiltonian in the momentum space would loose the easy expression $v_F\ \boldsymbol{\sigma}\cdot\mathbf{p}$ (the potential U generates a sum over all the possible momenta). In the following, we will show that the multiband Wigner procedure suggests a natural way to treat the Berry phases of the system for which there is no need to identify in the particle trajectory the "external parameter" of the Hamiltonian, as indicated by the previous artificial procedure. We define by $u_\pm$ the orthonormal eigenvectors of $\mathcal{H}_{g,a}=v_F\ \boldsymbol{\sigma}\cdot\mathbf{p}$. With the Dirac notation

$$\mathcal{H}_{g,a}(\mathbf{p})\left|u_\pm(\mathbf{p})\right\rangle=\pm v_F|\mathbf{p}|\left|u_\pm(\mathbf{p})\right\rangle \tag{52}$$

we write the solution of the Schrödinger problem

$$i\hbar\frac{\partial\left|\psi\right\rangle}{\partial t}=\mathcal{H}_{g,a}\left|\psi\right\rangle \tag{53}$$

as $\left|\psi\right\rangle=c_+(t)\left|u_+(\mathbf{p})\right\rangle+c_-(t)\left|u_-(\mathbf{p})\right\rangle$. A straightforward calculation gives (similar equation hold true for c_-)

$$i\hbar\frac{\partial c_+(t)}{\partial t}=-c_+(t)\left\langle u_+(\mathbf{p})\right|\frac{\partial u_+(\mathbf{p})}{\partial t}\left\rangle-c_-(t)\right\langle u_+(\mathbf{p})\left|\frac{\partial u_-(\mathbf{p})}{\partial t}\right\rangle+c_+(t)v_F|\mathbf{p}|\,. \tag{54}$$

The adiabatic theory ensures that the second term on the right side of the equation becomes arbitrarily small in the limit of sufficiently slow-in-time evolution of the momentum $\mathbf{p}$ (quasi-static or adiabatic hypothesis). An introduction to the adiabatic theory containing a

rigorous proof of this statement presented in a general context, can be found in (Teufel, 2003). If we assume the initial condition $|\psi(t_0)\rangle = |u_+(\mathbf{p})\rangle$, in the adiabatic limit Eq. (54) gives

$$|\psi(t)\rangle = |u_+(\mathbf{p}(t))\rangle \; e^{i\gamma_+(t) - \frac{i}{\hbar}\int_{t_0}^{t} v_F|\mathbf{p}(t')|\,\mathrm{d}t'} \;, \tag{55}$$

where the term γ_+ is denoted as dynamical phase factor. It can be evaluated by the path integral, along the $\mathbf{p}(t)$-trajectory of the Berry connection $\mathbf{A}(\boldsymbol{\xi})$

$$\gamma_+ = \int \mathbf{A}_{++}(\mathbf{p}) \cdot \,\mathrm{d}\mathbf{p} \;. \tag{56}$$

The Berry connection is given by

$$\mathbf{A}_{rs}(\mathbf{p}) = i\left\langle u_r(\mathbf{p})|\nabla_{\mathbf{p}} u_s(\mathbf{p})\right\rangle \quad ; \quad r,s = +,- \;. \tag{57}$$

According to the discussion presented in sec. 3.2, the multiband Wigner-Weyl formalism describes the particle motion by the set of equations (28)-(31)-(32). In order to see the connection with the Berry phase theory, it is useful to explore the classical limit, or $\hbar$-expansion of the Wigner-Weyl system. According to Eq. (19), if the external electric potential $U(\mathbf{r})$ is sufficiently regular, we have

$$\left[\Lambda(\mathbf{p}), \mathcal{S}'\right]_\star + \left[\mathcal{U}', \mathcal{S}'\right]_\star = \left[\mathfrak{A}, \mathcal{S}'\right] - \frac{i\hbar}{2}\left\{\nabla_{\mathbf{p}}\Lambda, \nabla_{\mathbf{r}}\mathcal{S}'\right\} + i\hbar\nabla_{\mathbf{r}}U \cdot \nabla_{\mathbf{p}}\mathcal{S}' + o(\hbar^2) \;, \tag{58}$$

where curly brackets denote the anti-commutators. We focus our attention to the first term of Eq. (58). In particular, $\mathfrak{A}$ groups all the terms that, originated from the $\hbar$-expansion procedure, are simple matrix multiplications acting on $\mathcal{S}'$ (all the other are differential operators):

$$\begin{aligned}\mathfrak{A} &= \Lambda + \frac{i\hbar}{2}\left[\Theta, \nabla_{\mathbf{p}}\Theta\right] \cdot \nabla_{\mathbf{r}}U \\ &= \begin{pmatrix} v_F|\mathbf{p}| & 0 \\ 0 & -v_F|\mathbf{p}| \end{pmatrix} + \frac{i\hbar}{2}\begin{pmatrix} \mathbf{A}_{++} & \mathbf{A}_{+-} \\ \mathbf{A}_{-+} & \mathbf{A}_{--} \end{pmatrix} \cdot \nabla_{\mathbf{r}}U \end{aligned} \tag{59}$$

In Eq. (59) we used that the columns of Θ are the eigenvectors of $\mathcal{H}$ (Eq. (24)) and by applying the definition of Eq. (57), we obtain $\mathbf{A}_{ij}(\mathbf{p}) = \left[\Theta(\mathbf{p})\nabla_{\mathbf{p}}\Theta(\mathbf{p})\right]_{ij} = \sum_k \Theta_{ik}\nabla_{\mathbf{p}}\Theta_{kj}$. Equation (59) emphasizes the role played by the Berry connection in the kinetic description of the particle-hole motion. In our formalism, the Berry connection leads to the first correction (in terms of an $\hbar$ expansion) of the classical of motion. Up to the first order in $\hbar$, the equations of motion (28) become (the components of $\mathcal{S}'$ are defined in Eq. (30))

$$\frac{\partial f^{\pm}}{\partial t} = \pm v_F \frac{\mathbf{p}}{|\mathbf{p}|} \cdot \nabla_{\mathbf{r}} f^{\pm} + \nabla_{\mathbf{r}}U \cdot \nabla_{\mathbf{p}} f^{\pm} \pm i\left(\mathcal{B}f^i - \overline{\mathcal{B}f^i}\right), \tag{60}$$

$$\frac{\partial f^i}{\partial t} = i\mathcal{A}f^i + \nabla_{\mathbf{r}}U \cdot \nabla_{\mathbf{p}} f^i + i\overline{\mathcal{B}}\left(f^+ - f^-\right), \tag{61}$$

where overbar means conjugation and

$$\mathcal{A} = -\frac{2v_F}{\hbar}|\mathbf{p}| + \frac{1}{2}\left(\mathbf{A}_{++} - \mathbf{A}_{--}\right) \cdot \nabla_{\mathbf{r}}U = -\frac{2v_F}{\hbar}|\mathbf{p}| + \frac{1}{|\mathbf{p}|^2}\left(\mathbf{p} \wedge \nabla_{\mathbf{r}}U\right)_z \;, \tag{62}$$

$$\mathcal{B} = \frac{1}{2}\mathbf{A}_{-+} \cdot \nabla_{\mathbf{r}}U = \frac{1}{2}\frac{p_x + ip_y}{|\mathbf{p}|^3}\left(\mathbf{p} \wedge \nabla_{\mathbf{r}}U\right)_z \;. \tag{63}$$

Here, $(\mathbf{p} \wedge \nabla_{\mathbf{r}} U)_z$ denotes the out-of-plane component (z-coordinate) of the vector $\mathbf{p} \wedge \nabla_{\mathbf{r}} U$. We remark that we use a slightly generalized definition of Berry connection. The standard Berry theory limits itself to consider the "in band" evolution of the system. This is a direct consequence of the adiabatic approximation that forbids band transitions. The Wigner-Weyl formalism, being more general, is not limited to any adiabatic hypothesis and band transition are allowed. For that reason, besides the diagonal Berry connections $\mathbf{A}_{++}$ and $\mathbf{A}_{--}$, the terms $\mathbf{A}_{+-}$ and $\mathbf{A}_{-+}$ appear. They are responsible for the particle band transitions (see the discussion of this point in (Morandi & Schürrer, 2011)).

5. Approximated model for the Wigner dynamics

The numerical solution to the equation of motion for the Wigner quasi-distribution function has been the subject of many studies (see i.e. (Frensley, 1990)). Often, a strong the similarity of the shape of the Wigner function with the classical counterpart can be observed. This is especially true in situations where strong quantum interference effects are not expected, but sometime also in the presence of sharp barriers and resonant structures. This consideration is often invoked for justifying the approximation of the θ operator appearing in Eq. (2) with the classical force term (leading term in the $\hbar$-expansion). Although the $\hbar$-expansion appears to be the most natural way to proceed, its application encounter many difficulties when approximations beyond the classical term are concerned. In fact, when applied to realistic problems, this procedure could generate a proliferation of corrective terms. Their number could be quite large and, furthermore, it is usually very difficult (sometime impossible) to ascribe to each term a clear physical meaning. Moreover, the range of validity of such an expansion, when truncated at a certain order, is questionable. The reason is that, at the microscopic level, the particle motion is characterized by complex phase-interference phenomena, which cannot be viewed as a simple refinement of the classical dynamics. Here, we present a slightly different strategy for approximating the Wigner equation of motion. The idea is to replace the θ operator, which is the source of the difference between classical and quantum dynamics, with a more tractable term. The similitude with the classical motion is exploited by approximating the Wigner evolution equation with a Liouville-like equation, where the force operator is the "best classical" approximation of the θ operator in the sense of the $\mathbf{L}^2$ norm. We consider the functional

$$\mathcal{N}[f] = \left\| \theta[f] - \mathbf{F}(\mathbf{r}) \frac{\partial f}{\partial \mathbf{p}} \right\|_{\mathbf{L}^2(\mathbb{R}^d_{\mathbf{r}} \times \mathbb{R}^d_{\mathbf{p}})} .$$

Here, the Wigner function is considered as a given function and the pseudo-field $\mathbf{F}$ is the unknown. We choose $\mathbf{F}$ such that the previous functional reaches the minimum value. The function $\mathbf{F}(\mathbf{r}, \mathbf{p})$ thus provides the closest approximation of $\theta[f]$ in the $\mathbf{L}^2(\mathbb{R}^d_{\mathbf{r}} \times \mathbb{R}^d_{\mathbf{p}})$ norm, for each function f sufficiently regular. The minimization of $\mathcal{N}[f]$ is obtained by solving the variational problem

$$\delta_{\mathbf{F}} \mathcal{N}[f] = 0 .$$

Straightforward calculations show that the minimizing function $\mathbf{F}$ is given by

$$F_j(\mathbf{r}) = -i \frac{\int_{\mathbb{R}^d_{\boldsymbol{\eta}}} \eta_j \mathcal{D}(\mathbf{r}, \boldsymbol{\eta}) \left| \widetilde{f}(\mathbf{r}, \boldsymbol{\eta}) \right|^2 \mathrm{d}\boldsymbol{\eta}}{\int_{\mathbb{R}^d_{\boldsymbol{\eta}}} \eta_j^2 \left| \widetilde{f}(\mathbf{r}, \boldsymbol{\eta}) \right|^2 \mathrm{d}\boldsymbol{\eta}} . \tag{64}$$

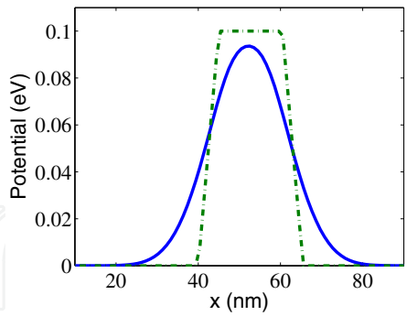

(a) Green dot dashed line: external potential. Blue continuous line: pseudo-potential

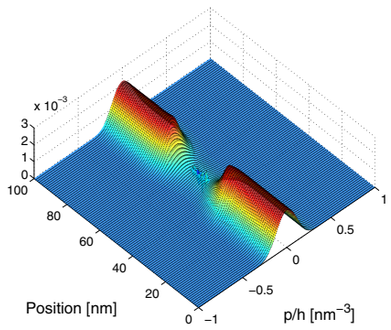

(b) Quantum-corrected distribution.

Fig. 4. Comparison between the external potential U and the pseudo-potential $U^* = \int \mathbf{F}\, \mathrm{d}\mathbf{r}$.

Equation (64) reveals that the calculation of the pseudo-force field in a certain position requires the knowledge of the potential in the overall $\mathbf{r}$ space (via the term $\mathcal{D}$). By computing the integral, the potential U is evaluated at the positions $\mathbf{r} \pm \frac{\hbar}{2}\boldsymbol{\eta}$ and has a measure proportional to $\left|\widetilde{f}\right|^2$, the spectral power of f in the $\boldsymbol{\eta}-$space. As a consequence, the more the $\mathbf{p}$-gradient of the solution $f(\mathbf{r}, \mathbf{p})$ increases, the more the force $\mathbf{F}$ becomes non-local and the values of the potential faraway from $\mathbf{r}$ are important. This can be expressed pictorially by saying that, as compared with a smoother distribution function, an irregular profile of the solution "sees" a larger spatial region. The approximated quantum-Wigner evolution equation becomes

$$\frac{\partial f}{\partial t} = -\frac{\mathbf{p}}{m} \cdot \nabla_{\mathbf{r}} f - \mathbf{F}(\mathbf{r}) \cdot \nabla_{\mathbf{p}} f \,. \tag{65}$$

This is a nonlinear system where the pseudo-electric field $\mathbf{F}$ depends on the solution itself. In some situations, the nonlinearity can be eliminated and a good approximation of the field $\mathbf{F}$ can be obtained by replacing in Eq. (64) the solution f with the classical Boltzmann equilibrium distribution at the temperature T

$$f^{eq} = \sqrt{\frac{mkT}{\pi}} e^{-\frac{1}{kT}\left(\frac{|\mathbf{p}|^2}{2m} - \mu\right)} \,,$$

where μ is the chemical potential of the particle gas and k the Boltzmann constant. In fig. 4 the comparison of the classical and the pseudo electric field obtained by using the Boltzmann distribution function is presented. A glance at the figure reveals that, compared with the bare potential U, the effective pseudo-potential is smoother and extends beyond the support of U. As a consequence, the particle in the presence of the quantum corrected potential are decelerated or accelerated before they reach the classical force field $-\nabla_{\mathbf{r}} U$, making evident the non-local action of the quantum potential. Furthermore, the snapshot fig. 4-(a) shows that the maximum value of the effective potential is smaller than the classical one. As a consequence, particles with energy smaller than the maximum of the potential (but greater than the maximum of the pseudo-potential) are not reflected by the barrier. This simple example illustrates how quantum tunneling can be approximatively described by a classical formalism. Furthermore, in fig. 4-(b) we depict the solution of Eq. (65) in the presence of the potential U. At the boundary, the Boltzmann distribution is imposed.

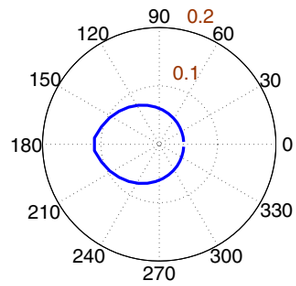

(a) Initial condition.

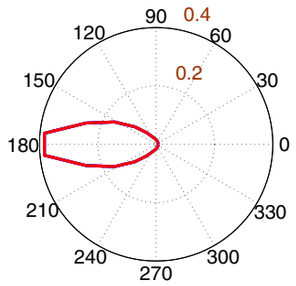

(b) $t = 0.3$ ps.

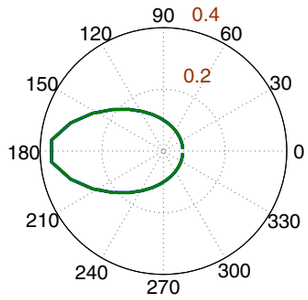

(c) $t = 10$ ps.

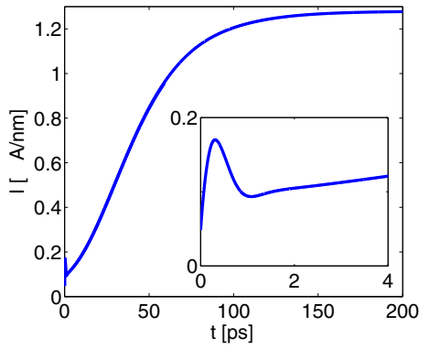

(d) Time evolution of the total current.

Fig. 5. (a)-(c) Polar plot of the density for current in graphene. (d) Total current.

6. Dissipative effects in the Wigner formalism: electron-phonon collisions in graphene

As described in the introduction, one of the major advantages of the Wigner formalism is the possibility to include in a quantum mechanical treatment also some dissipative effects, or (in the opposite limit) to derive some quantum corrected models for the simulation of quasi-classical systems. As an example, we apply the results obtained in sec. 5 for studying the particles evolution in graphene and we include a detailed description of the electron-phonon scattering phenomena, via a Boltzmann scattering collision operator. An important property of the pseudo-electric field approximation is the preservation of the positivity of the quantum-corrected distribution function. Since the Boltzmann collision operator is defined only for positive functions, positivity preservation becomes a fundamental property for any Boltzmann quantum-corrected kinetic model (anyway, despite the lack of theoretical support, some Wigner-Boltzmann solver have been numerically tested (Kosina & Nedjalkov, 2006)). A semiclassical Boltzmann model with quantum corrections, allows the study of the relaxation processes dynamically, providing information on the time scale on which the equilibrium is established.

The phonon system of graphene has already been thoroughly investigated by means of density functional theory (DFT) and Raman spectroscopy (Piscanec et al., 2004). The phonon dispersion relations and electron-phonon coupling matrix elements are essential ingredients for kinetic models of carrier transport in graphene. Results of DFT calculations show that longitudinal optical (LO) and transversal optical (TO) phonons modes contribute significantly

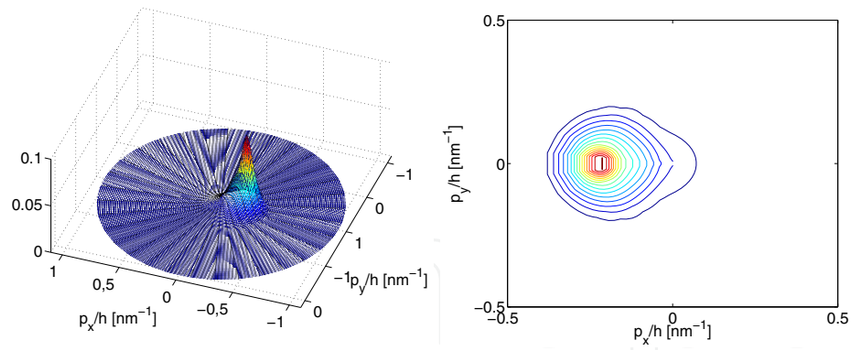

(a) $t = 0.3$ ps.

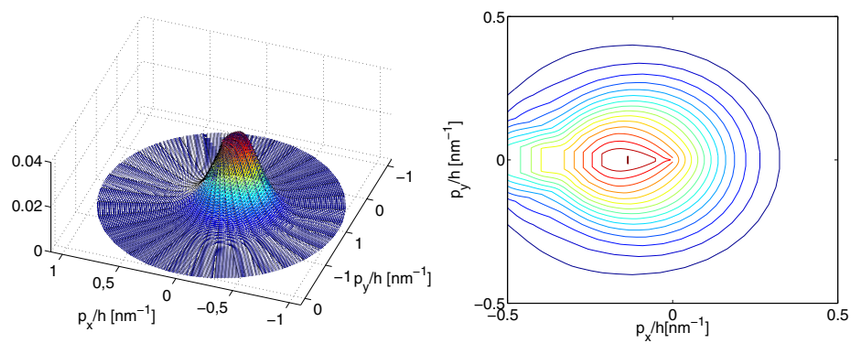

(b) $t = 1$ ps.

Fig. 6. 3D and contour plot representation of the f^+ distribution for different times.

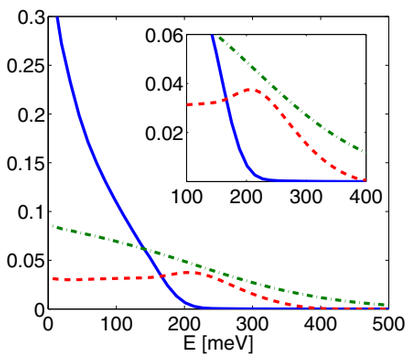

(a) Evolution of the energy density for $t = 0$ (continuous blue line), $t = 0.3$ ps (dashed red line) $t = 10$ ps (dot-dashed green line).

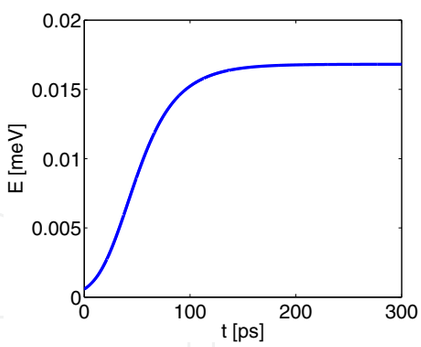

(b) Total energy of the system.

Fig. 7. Evolution of the energy density and the total energy of the particle gas.

to inelastic scattering of electrons in graphene. Because of their short wave vectors these phonons scatter electrons within one valley. In addition, zone boundary phonons close to the **K**-point are responsible for intervalley processes. The Boltzmann equation of motion

including optical phonon scattering writes

$$\frac{\partial f^{\pm}}{\partial t} \mp v_F \frac{\mathbf{p}}{|\mathbf{p}|} \cdot \nabla_{\mathbf{r}} f^{\pm} - \mathbf{F} \cdot \nabla_{\mathbf{p}} f^{\pm} = \sum_{\eta,j} \mathcal{C}^{\eta}_{\pm j} \,. \tag{66}$$

The collision kernel, containing emission and absorbtion processes, is given by

$$\mathcal{C}^{\eta}_{ij}(\mathbf{p}) = \frac{1}{(2\pi)^2} \int_{\mathcal{B}} \left\{ W^{\eta}_{\mathbf{p}'_j \mathbf{p}^i} f^j(\mathbf{p}')[1 - f^i(\mathbf{p})] - W^{\eta}_{\mathbf{p}^i \mathbf{p}'_j}[1 - f^j(\mathbf{p}')] f^i(\mathbf{p}) \right\} \mathrm{d}\mathbf{p}' \,, \quad i,j = \pm \tag{67}$$

where η labels the specific scattering processes, $\mathcal{B}$ denotes the first Brillouin zone of graphene and

$$W^{\eta}_{\mathbf{p}^i \mathbf{p}'^j} = s^{\eta}_{\mathbf{p}'_j \mathbf{p}^i} \, \left[1 + g_\eta(\boldsymbol{p} - \boldsymbol{p}')\right] \, \delta(\varepsilon_i - \varepsilon'_j - \hbar\omega_\eta) + s^{\eta}_{\mathbf{p}^i \mathbf{p}'^j} \, g_\eta(\boldsymbol{p}' - \boldsymbol{p}) \, \delta(\varepsilon_i - \varepsilon'_j + \hbar\omega_\eta) \,. \tag{68}$$

The delta functions (where we adopt the simplified notation $\varepsilon_i = \varepsilon_i(\boldsymbol{p})$, $\varepsilon'_j = \varepsilon_j(\boldsymbol{p}')$ and ω_η denotes the energy of the η-th mode) ensure the conservation of the energy during the scattering processes. The explicit expression of the scattering elements $s^{\eta}_{\mathbf{p}'_j \mathbf{p}^i}$, can be found in (Lichtenberger et al., 2011; Piscanec et al., 2004). According to sec. 3.2, the functions f^+ and f^- represent the particle distribution in the upper and in the lower Dirac cone, respectively. Finally, the g_η are the phonon equilibrium distribution functions related to the η-th mode. Here, for sake of simplicity, we assume that the phonon system is an infinite reservoir at a constant temperature T. In this hypothesis, the g_η can be approximated by the Bose-Einstein distributions $g^0_\eta = [\exp(\hbar\omega_\eta / k_B T) - 1]^{-1}$. The study of the coupled electron-phonon system is presented in (Lichtenberger et al., 2011). It has been shown that the optical phonons are in equilibrium only for a low-bias polarization (around 0.1 eV), otherwise hot phonon effects should be included.

We apply the Boltzmann system given in Eq. (66) to study the transient evolution of the electron-hole and phonon gas in response on the abrupt change of the applied bias. As initial datum, for $t = 0$, we assume that the graphene sheet is in the stationary state for an applied voltage U equal to 0.01 V. For $t > 0$ we impose $U = 0.1$ V. In Fig. 5-d we show the evolution of the total current at the drain contact for the intrinsic graphene. The simulations reveal the presence of a current overshoot (approximatively one picosecond after the potential change) and a subsequent approach to the equilibrium value. The further approach to the equilibrium is a quite slower process of approximatively 200 picoseconds.

The detailed explanation of the transient current overshoot observed during the first picosecond requires a deeper analysis of the high non-equilibrium motion of the hot carriers. The presence of an overshoot in the current evolution is an unexpected phenomenon in graphene. It is well known that, in this material, the carrier velocity is independent from the modulus of the momentum. For this reason, we expect that even if some transient phenomena are able to move the hot carriers toward high values of the momentum, this should not significantly affect their velocity and consequently the total current of the system. The overshoot can be explained by analyzing the following two-step process: initially the particles are ballistically accelerated by the strong external field (the temperature of the particles gas stays essentially constant). However, after some picoseconds, the scattering processes are able to transform the kinetic energy of the carriers into thermal energy. During the first picosecond, the component of the momentum parallel to the external field increases. As a consequence, the direction of the momentum (and thus the velocity) is turned toward the direction of the

electric field. In this first part of the dynamics, the motion is essentially ballistic, the particles share similar momentum direction and group together in the velocity space. This behaviour is evident from fig. 5 where we depict the polar plot of the angular density of the current. For $t < 0.3$ ps the drift term dominates the Boltzmann collision operator. The latter is a nonlinear operator and its effects on the distribution function depend on the shape of the function itself. On the contrary, the ballistic operator translates the distribution function over the phase plane along the Hamiltonian flux and is independent of the distribution. During the overshoot of the current, the Boltzmann operator is not able to balance the effect of the ballistic term. This can be seen in fig. 6 where we depict the evolution of the electron distribution function f^+ for different times. The first part of the dynamics (fig. 6(a)) is just a rigid translation of f^+ towards higher values of the momentum variable. After one picosecond, an enlargement of the distribution function around its center of mass can be observed. This is a clear signature of the temperature increase of the system. The friction process occurs only by dissipating the kinetic energy of the particles by phonon emission. This requires a certain time delay. A closer look at the density of energy of the carriers explains the reason why the particle gas need a delay before starting to emit phonons. In fig. 7 we plot the evolution of the energy density and the total energy of the particles. We see that a peak of high energy particles is present after 0.3 ps. This peak represents the particles accelerated by the field. Their kinetic energy increases until they are able to emit optical phonons (whose energy is 196 and 161 eV for Γ and **K** phonons respectively). Around an energy of 200 meV, the kinetic energy can be efficiently dissipated and the distribution reaches a new thermal-like state characterized by a smaller total current.

6.1 Conclusions

In this Chapter, various approaches based on the Wigner-Weyl formalism, are presented. In particular, we highlight the existence of a general formalism where in analogy with the Schrödinger formalism, we use the class of unitary operators in order to define a class of equivalent quasi-distribution functions. The applications of this formalism span among different subjects: the multi-band transport in nano-devices, the infinite-order $\hbar$-approximations of the motion and the characterization of a system in terms of Berry phases or, more generally, the representation of a quantum system by means of a Riemann manifold with a suitable connection. The exposition of the theory is completed with some numerical test and applications to real devices.

7. Acknowledgment

The research was founded by the Austrian Science found (FWF): P21326-N16.

8. References

Alvaro, M. & Bonilla, L. L., (2010). Two miniband model for self-sustained oscillations of the current through resonant-tunneling semiconductor superlattices, *Phys. Rev. B* Vol. 82, 035305.

Arnold, A, (2008). Mathematical properties of quantum evolution equations. In: G. Allaire, A. Arnold, P. Degond, and T. Hou (eds.), *Quantum Transport - Modelling, Analysis and Asymptotics, Lecture Notes Math.* 1946, 45-110. Springer, Berlin.

Beenakker, C. W. J., Akhmerov, A. R., Recher, P. & Tworzydło, J., (2008). Correspondence between Andreev reflection and Klein tunneling in bipolar graphene, *Phys. Rev. B* Vol. 77, 075409.

Bohm, A., Mostafazadeh, A., Koizumi, H., Niu, Q. & Zwanziger, J., (2008). *The Geometric Phase in Quantum Systems: Foundations, Mathematical Concepts, and Applications in Molecular and Condensed Matter Physics*, Sringer-Verlag (Berlin, Heideberg).

Cohen, L., (1966). Generalized phase-space distribution functions, *Journal of Mathematical Physics* Vol. 7, 781.

Demeio, L., Bordone, P. & Jacoboni, C., (2006). Multi-band, non-parabolic Wigner-function approach to electron transport in semiconductors, *Transp. Theory Stat. Phys.*, Vol. 34, 1.

Folland, G. B., (1989). *Harmonic Analysis in Phase Space*, Princeton University Press, Princeton.

Frensley, W. R. (1990). Boundary conditions for open quantum driven far from equilibrium, *Rev. Mod. Phys.* Vol. 62 (No. 3), 745.

Giulini, W., Joos, E., Kiefer, C., Kupsch, J., Stamatescu, I.-O., Zeh, H. D., (2003). *Decoherence and the appearance of a classical world in quantum theory* Springer-Verlag Berlin.

Jüngel, A., (2009). *Transport Equations for Semiconductors*, Springer-Verlag, Berlin.

Kosina H. & Nedjalkov, M., (2006). Wigner function-based device modeling. In: M. Rieth and W. Schommers (eds), Handbook of Theoretical and Computational Nanotechnology 10, 731.

Lee, H.-W. (1995). Theory and application of the quantum phase-space distribution functions, *Physics Reports*, Vol. 259, 147.

Lions, P.-L. & Paul, T. (1993). Sur les mesures de Wigner. *Rev. Mat. Iberoamer*, Vol. 9, 553.

Lichtenberger, P., Morandi, O. & Schuerrer, F., (2011). High field transport and optical phonon scattering in graphene, *Phys. Rew. B*, Vol. 84, 045406.

Markowich, P., Ringhofer, C. & Schmeiser, C. (1990). *Semiconductor Equations.* Wien: Springer Verlag.

Markowich, P. & Ringhofer, C. (1989). An analysis of the quantum Liouville equation. *Z. Angew. Math. Mech.*, Vol. 69, 121.

Morandi, O., Modugno, M. (2005). A multiband envelope function model for quantum transport in a tunneling diode. *Phys. Rev. B*, Vol. 71, 235331.

Morandi, O. & Demeio, L., (2008). A Wigner-function approach to interband transitions based on the multiband-envelope-function model, *Transp. Theory Stat. Phys.*, Vol. 37, 437.

Morandi, O. (2009). Multiband Wigner-function formalism applied to the Zener band transition in a semiconductor, *Phys. Rev. B* Vol. 80, 024301.

Morandi, O., (2010). A WKB approach to the quantum multiband electron dynamics in the kinetic formalism, *Communications in Applied and Industrial Mathematics*, Vol. 1, 474.

Morandi, O., (2010). Effective classical Liouville-like evolution equation for the quantum phase space dynamics, *J. Phys. A: Math. Theor.* Vol. 43, 365302.

Morandi, O. & Schuerrer, F. (2011). Wigner model for quantum transport in graphene, *J. Phys. A: Math. Theor*, Vol. 44, 265301.

Morandi, O. & Schuerrer, Wigner model for Klein tunneling in graphene, *Communications in Applied and Industrial Mathematics*, in publication.

Morandi, O., Barletti, L. & Frosali, G. Perturbation Theory in terms of a generalized phase Quantization procedure, *Boll. Unione Mat. Ital.*, Vol. 4 (No. 1), 1.

Castro Neto, A. H., Guinea, F.,Peres, N. M. R., Novoselov K. S., & Geim, A. K. (2009). The electronic properties of graphene, *Rev. Mod. Phys.*, Vol. 81, 109.

Piscanec, S., Lazzeri, M., Mauri, F., Ferrari, A. C. and Robertson, J., (2004). Kohn Anomalies and Electron-Phonon Interactions in Graphite, *Phys. Rev. Lett.*, Vol. 93, 185503.

Teufel, S., (2003). *Adiabatic Perturbation Theory in Quantum Dynamics*. Springer-Verlag Berlin.

Unlu, M. B., Rosen B., Cui, H.-L. & Zhao, P., (2004). Multi-band Wigner function formulation of quantum transport, *Phys. Lett. A* Vol. 327, 230.

Wigner, E. (1932). On the quantum correction for thermodynamic equilibrium, *Phys. Rev.*, Vol 40, 749.

Xiao, D., Chang, M.-C., & Niu, Q., Berry phase effects on electronic properties, *Rev. Mod. Phys.*, Vol. 82, 1959.

Zachos, C. K., Fairlie, D. B., & Curtright T. L. (editors), (2005). *Quantum mechanics in phase space. An overview with selected papers*. World Scientific Publishing: Hackensack (NJ).

Zener, C. (1934). A Theory of the Electrical Breakdown of Solid Dielectrics, *Proc. R. Soc. London, Ser. A* Vol. 145, 523.

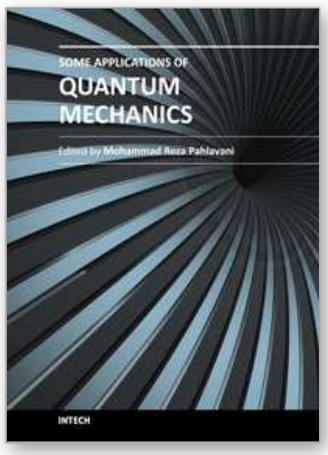

Some Applications of Quantum Mechanics

Edited by Prof. Mohammad Reza Pahlavani

ISBN 978-953-51-0059-1
Hard cover, 424 pages
Publisher InTech
Published online 22, February, 2012
Published in print edition February, 2012

Quantum mechanics, shortly after invention, obtained applications in different area of human knowledge. Perhaps, the most attractive feature of quantum mechanics is its applications in such diverse area as, astrophysics, nuclear physics, atomic and molecular spectroscopy, solid state physics and nanotechnology, crystallography, chemistry, biotechnology, information theory, electronic engineering... This book is the result of an international attempt written by invited authors from over the world to response daily growing needs in this area. We do not believe that this book can cover all area of application of quantum mechanics but wish to be a good reference for graduate students and researchers.

InTech Europe
University Campus STeP Ri
Slavka Krautzeka 83/A
51000 Rijeka, Croatia
Phone: +385 (51) 770 447
Fax: +385 (51) 686 166
www.intechopen.com

InTech China
Unit 405, Office Block, Hotel Equatorial Shanghai
No.65, Yan An Road (West), Shanghai, 200040, China
中国上海市延安西路65号上海国际贵都大饭店办公楼405单元
Phone: +86-21-62489820
Fax: +86-21-62489821

IntechOpen